

https://dspace.org/

Corpus callosum thickness on MRI as a surrogate marker of brain volume in children with HIV-related brain disease and its correlation with developmental scores

Andronikou, Savvas

2015

http://hdl.handle.net/10539/19628

Downloaded from a DSpace repository. https://dspace.org/

Corpus Callosum Thickness on MRI as a Surrogate Marker of Brain Volume in Children with HIV-Related Brain Disease and its Correlation with Developmental Scores

Savvas Andronikou

A research report submitted to the Faculty of Health Sciences, University of the Witwatersrand, Johannesburg, in fulfilment of the requirements for the degree of Doctor of Philosophy

Johannesburg, 2015

Declaration

I, Savvas Andronikou, declare that this research report is my own work. It is being submitted for the degree of PhD in the Faculty of Health Sciences at the University of the Witwatersrand, Johannesburg. It has not been submitted before for any degree or examination at this or any other University.



_____

Savvas Andronikou

On this 6th day of October 2015

I dedicate this work to my parents, Andreas and Andreoula Andronikou, who have understood the value of education in their own lives and instilled a passion for it in mine. I thank them for their self-sacrifice during refugee years of struggle to give us the best education possible.

I also dedicate this work to my close friend Andrew Nathaniel who was an academic at heart, but who succumbed to a disease himself.

Publications and presentations

This work has been published in a number of papers as listed below:

Publications

1. Ackermann C, Andronikou S, Laughton B, Kidd M, Dobbels E, Innes S, et al. White matter signal abnormalities in children with suspected HIV-related neurologic disease on early combination antiretroviral therapy. Pediatr Infect Dis J. 2014;33:e207-212. [Appendix A] [Equal contribution to the first author in conceiving the project, collecting data and writing – see letter by Dr Ackerman appendix B]
2. Andronikou S, Spottiswoode B, S., Tomazos N. A semi-automated method for measuring thickness and white matter integrity of the corpus callosum. South African Journal of Radiology. 2012;16:130-133. [Appendix C]
3. Andronikou S, Pillay T, Gabuza L, Mahomed N, Naidoo J, Hlabangana L T, et al. Corpus callosum thickness in children: an MR pattern-recognition approach on the midsagittal image. Pediatr Radiol. 2015;45:258-272.[Appendix D]
4. Andronikou S, Ackermann C, Laughton B, Cotton M, Tomazos N, Spottiswoode B, et al. Correlating brain volume and callosal thickness with clinical and laboratory indicators of disease severity in children with HIV-related brain disease. Childs Nerv Syst. 2014;30:1549-1557. [Appendix E]
5. Andronikou S, Ackermann C, Laughton B, Cotton M, Tomazos N, Spottiswoode B, et al. Corpus callosum thickness on mid-sagittal MRI as a marker of brain volume: a pilot study in children with HIV-related brain disease and controls. Pediatr Radiol. 2015;45:1016-1025. [Appendix F]

Presentations:

Andronikou S, Ackermann C, Laughton B, Dobbels E, Innes S, Taliep R, van Toorn R, Cotton M, Spottiswoode B, Pettifor J. Corpus Callosum Thickness on MRI as a Surrogate Marker of White Matter Volume in Children with HIV and its Correlation with Developmental Scores. Oral Presentation European Society of Pediatric Radiology 2012, 28 May – 1st June 2012, Athens, Greece 2012 [Appendix G]

Spottiswoode B, **Andronikou S**. Division of the Corpus Callosum into multiple points for measuring thickness and generating fiber tracts – a semi-automated method for determining normal values and for use as a surrogate marker of hemispheric disease. Poster presentation ESPR 2010, 7-11 June 2010, Bordeaux France [Appendix H]

Abstract

Background

Objective volumetric assessment of white matter in children with HIV involves post-processing, while corpus callosum (CC) thickness measurement on mid-sagittal MRI may represent a rapid surrogate marker.

Aim

To determine whether the thickness of the CC on mid-sagittal MRI can be used as a surrogate marker of brain volume in children with HIV-related brain disease and in appropriate controls and to determine whether thickness at particular locations correlates with mental developmental scores and laboratory markers of immunity.

Methods

A retrospective analysis of 33 children with HIV-related neurology (range 7 - 49 months; median 31 months; mean 30 months; 16 boys and 17 girls) and matched controls (range 13 – 48 months; median 34 months; mean 32 months; 6 boys and 5 girls) was performed. A custom software tool imported sagittal MRI images, divided the midline CC contour into 40 segments and measured the thickness of each segment as well as the length of the CC. Brain volume (total brain volume (TBV); white matter volume (WMV); grey matter volume (GMV)) was determined using MATLAB and Statistical Parametric Mapping software. Overall and segmental CC mean and maximum thickness and CC length were checked for correlation with brain volume, Griffiths mental development scores (GMDS) and laboratory parameters.

Results

Griffiths scores in patients were 'low average' (mean Griffiths general quotient (GQ) of 84, range 72 – 101; 'locomotor' 84, range 59 – 116; 'language' 80; range 57 – 118).

There was no statistical difference in overall and regional CC thickness, CC length, TBV, GMV and WMV between patients and controls.

Significant correlation was found in patients for the premotor CC mean with age (p = 0.04). Other significant correlations of CC measurements and laboratory / clinical parameters were the prefrontal CC max with nadir CD4 (p=0.046)(+ve correlation); motor CC max with GQ (p=0.028) (-ve correlation) and CC length with CD4 (p=0.04) (-ve correlation).

Significant correlations between CC thickness and brain volume were found in patients and controls for the CC mean and TBV (p=0.049)(+ve correlation); premotor CC mean and TBV (p=0.039)(+ve correlation); sensory CC mean and TBV (p=0.022)(+ve correlation); prefrontal CC max and WMV (p=0.019)(+ve correlation); premotor CC mean and WMV (p=0.019)(+ve correlation and for the premotor CC max and WMV (p=0.023)(+ve correlation).

Conclusion:

This research met its objectives in demonstrating a statistically significant, albeit weak, correlation between CC thickness and brain volume in patients and controls, even though patients were not shown to have significantly diminished brain volumes as compared to controls.

Although the maximum thickness of the prefrontal segment of the CC also showed a statistically significant correlation with nadir CD4 (which is the lowest point of immunity measured for a patient), we have not demonstrated significant clinical usefulness of for CC thickness in our patients.

Acknowledgements

I acknowledge assistance with the digital software development (Bruce Spottiswoode), software application (Nicollette Tomazos) and statistical assistance (Katya Mauf, Elena Liebhaber and Martin Kidd). I also thank Bruce Spottiswoode for all his assistance as a technical co-supervisor and for giving his time to perform second reader measurements for the study.

I acknowledge the radiological assistance and insights of Christelle Ackermann of the Radiology Department at the University of Stellenbosch, South Africa, in collecting the case material and conceiving numerous research projects, including this one, in which we are both invested.

I also acknowledge the clinical assistance of Barbara Laughton, Els Dobbels, Steve Innes, Reghana Taliep, Ronald van Toorn and Mark Cotton of the Children's Infectious Diseases Research Unit, University of Stellenbosch and Tygerberg Children's Hospital, South Africa and the Department of Paediatrics and Child Health, University of Stellenbosch, South Africa.

I thank Susan Lucas for assisting me with my thesis formatting and proof reading and I also thank her for her efforts in developing document templates for our whole department to benefit from.

I give my sincere thanks to my supervisor Prof John Pettifor. His persistence as well as his insistence on detail and accuracy led me safely to the end.

Table of Contents

Declaration ii

Publications and presentations iv

Abstract vi

Acknowledgements ix

Table of Contents x

List of Figures xv

List of Tables xx

List of Abbreviations xxii

1. Introduction 1

1.1. Hypothesis 1

1.2. Justification of the research question 1

1.3. Study Aim 2

1.4. Study Objectives 2

1.5. Preview and Organisation of the Thesis 3

1.6. Literature Review 6

1.6.1 Definition and function of the corpus callosum 6

1.6.2 Development and variability of the corpus callosum 6

1.6.3 Functional units of the corpus callosum 7

1.6.4 Corpus callosum thickness 9

1.6.5 Correlating corpus callosum size with disease and performance 10

1.6.6 CNS imaging in children with HIV and its effects on brain volume 13

1.6.7 MRI Volumetric techniques 14

1.6.8 Corpus callosum in HIV 15

1.6.9 Corpus callosum thickness and brain volume in HIV in the HAART era 17

1.6.10 How the current research has arisen from the failures / inadequacies of previous work 18

2. Materials and Methods 19

2.1. Study Design 19

2.2. Study Setting 19

2.3. Study Population 19

2.4. Sampling 21

2.5. Inclusion Criteria 21

2.6. Exclusion Criteria 21

2.7. Measurement Instruments 22

2.7.1 CC thickness measurement 22

2.7.2 Brain volume calculation 24

2.8. Data 25

2.8.1 Overall mean and maximum CC thickness 25

2.8.2 Segmental CC mean and maximum thickness 25

2.8.3 CC length (from tip of rostrum midpoint to tip of splenium midpoint) 27

2.8.4 Brain volumes 27

2.8.5 Griffiths Mental Development Scores (GMDS) 27

2.8.6 Clinical and laboratory data 27

2.9. Data Analysis 28

2.10. Ethical Issues 29

3. Results 29

3.1. General results of corpus callosum thickness, corpus callosum length and brain volume 30

3.2. Results of clinical findings 43

3.2.1. Griffiths Mental Development Scores (GMDS) 43

3.2.2. Clinical and Laboratory Parameters 44

3.3. Results of comparison of patients with controls 46

3.4. Results of correlations of MRI features (corpus callosum thickness, length, brain volumes) with each other and with clinical / laboratory parameters 55

4. Discussion 63

4.1. Meeting the objectives of the study 63

4.1.1. Comparing corpus callosum thickness and brain volume in children with HIV-related brain disease against 'normal' children and determining which segments of the corpus callosum are most affected 63

4.1.2. Correlating corpus callosum thickness with brain volume in children with HIV-related brain disease 66

4.1.3. Correlating segmental prefrontal corpus callosum thickness with brain volume in children with HIV-related brain disease 67

4.1.4. Correlation of corpus callosum thickness with mental development scores in children with HIV-related brain disease 68

4.1.5. Correlation of corpus callosum thickness and brain volume with laboratory parameters of immunosuppression in children with HIV-related brain disease 69

4.1.6. The corpus callosum length and its relationship to clinical findings 69

4.1.7. HAART may be neurotoxic 70

4.1.8. Other studies of corpus callosum thickness measurement 71

4.2. Current applications 73

4.2.1 Semi-automated method of measuring corpus callosum thickness 73

4.3. Limitations of the current study 73

4.3.1. Sample limitations 73

4.3.2. Limitations relating to controls 74

4.3.3. Limitations to comparing with published research 75

4.3.4. Technical limitations of corpus callosum thickness measurement 75

4.3.5. Structural vs. physiological assessment 77

4.4. Future applications 77

5. Conclusion 79

Appendix A: White Matter Signal Abnormalities in Children With Suspected HIV-related Neurologic Disease on Early Combination Antiretroviral Therapy 80

Appendix B: Letter of contribution by first author 81

Appendix C: A semi-automated method for measuring thickness and white matter integrity of the corpus callosum 82

Appendix D: Corpus callosum thickness in children: an MR pattern-recognition approach on the midsagittal image 83

Appendix E: Correlating brain volume and callosal thickness with clinical and laboratory indicators of disease severity in children with HIV-related brain disease 84

Appendix F: Corpus Callosum Thickness on Mid-sagittal MRI as a Marker of Brain Volume: A pilot Study in Children with HIV Related Brain Disease and Controls 85

Appendix G: Oral Presentation Athens 2012 86

Appendix H: Poster ESPR 2010, 7-11 June 2010, Bordeaux France..... 87

Appendix I: Ethics clearance certificate 88

6. References..... 89

List of Figures

Figure 1.1. Sagittal T1 MRI image of central corpus callosum thinning (white arrows) corresponding to unilateral brain loss after excision of a left-sided tumour (black arrow) on T2, with a comparison sagittal T1 weighted image showing thickness of the corpus callosum in a normal child (Normal) 12

Figure 1.2. Sagittal T1 weighted image showing predominantly posterior corpus callosum thinning (long arrow) corresponding to predominantly posterior peri-ventricular leukomalacia (short arrows) on FLAIR after a perinatal hypoxic insult, with a comparison sagittal T1 weighted image showing thickness of the corpus callosum in a normal child (Normal) 12

Figure 1.3. Sagittal T2 showing generalised corpus callosum thinning related to global white matter volume loss after a global hypoxic event at birth as seen on axcial T2, with a comparison sagittal T1 weighted image showing thickness of the corpus callosum in a normal child (Normal) 12

Figure 2.1 a and b: corpus callosum thickness measurement: (a) Midline sagittal T1 weighted MRI indicating the 40 radial measurements of thickness produced by the custom-made semi-automated tool and (b) plotted along the length (diameter) of the corpus callosum automatically from start of the genu (at 0 mm) to the end of the splenium (at 50 mm). 24

Figure 2.2 a and b: (a) Annotated midline sagittal MRI demonstrating the predefined corpus callosum segments and (b) calculation of mean thickness by inclusion of all measurements within a segment..... 26

Figure 3.1. Patient 1- Sagittal T1, corpus callosum radial thickness measurements, thickness graph, GM and WM segmentation..... 34

Figure 3.2. Patient 2- Sagittal T1, corpus callosum radial thickness measurements, thickness graph, GM and WM segmentation..... 34
Figure 3.3. Patient 3- Sagittal T1, corpus callosum radial thickness measurements, thickness graph, GM and WM segmentation..... 34
Figure 3.4. Patient 4- Sagittal T1, corpus callosum radial thickness measurements, thickness graph, GM and WM segmentation..... 34
Figure 3.5. Patient 5- Sagittal T1, corpus callosum radial thickness measurements, thickness graph, GM and WM segmentation..... 35
Figure 3.6. Patient 6- Sagittal T1, corpus callosum radial thickness measurements, thickness graph, GM and WM segmentation..... 35
Figure 3.7. Patient 7- Sagittal T1, corpus callosum radial thickness measurements, thickness graph, GM and WM segmentation..... 35
Figure 3.8. Patient 8- Sagittal T1, corpus callosum radial thickness measurements, thickness graph, GM and WM segmentation..... 35
Figure 3.9. Patient 9- Sagittal T1, corpus callosum radial thickness measurements, thickness graph, GM and WM segmentation..... 36
Figure 3.10. Patient 10- Sagittal T1, corpus callosum radial thickness measurements, thickness graph, GM and WM segmentation..... 36
Figure 3.11. Patient 11- Sagittal T1, corpus callosum radial thickness measurements, thickness graph, GM and WM segmentation..... 36
Figure 3.12. Patient 12- Sagittal T1, corpus callosum radial thickness measurements, thickness graph, GM and WM segmentation..... 36
Figure 3.13. Patient 13- Sagittal T1, corpus callosum radial thickness measurements, thickness graph, GM and WM segmentation..... 37

Figure 3.14. Patient 14- Sagittal T1, corpus callosum radial thickness measurements, thickness graph, GM and WM segmentation..... 37
Figure 3.15. Patient 15- Sagittal T1, corpus callosum radial thickness measurements, thickness graph, GM and WM segmentation..... 37
Figure 3.16. Patient 16- Sagittal T1, corpus callosum radial thickness measurements, thickness graph, GM and WM segmentation..... 37
Figure 3.17. Patient 17- Sagittal T1, corpus callosum radial thickness measurements, thickness graph, GM and WM segmentation..... 38
Figure 3.18. Patient 18- Sagittal T1, corpus callosum radial thickness measurements, thickness graph, GM and WM segmentation..... 38
Figure 3.19. Patient 19- Sagittal T1, corpus callosum radial thickness measurements, thickness graph, GM and WM segmentation..... 38
Figure 3.20. Patient 20- Sagittal T1, corpus callosum radial thickness measurements, thickness graph, GM and WM segmentation..... 38
Figure 3.21. Patient 21- Sagittal T1, corpus callosum radial thickness measurements, thickness graph, GM and WM segmentation..... 39
Figure 3.22. Patient 22- Sagittal T1, corpus callosum radial thickness measurements, thickness graph, GM and WM segmentation..... 39
Figure 3.23. Patient 23- Sagittal T1, corpus callosum radial thickness measurements, thickness graph, GM and WM segmentation..... 39
Figure 3.24. Patient 24- Sagittal T1, corpus callosum radial thickness measurements, thickness graph, GM and WM segmentation..... 39
Figure 3.25. Patient 25- Sagittal T1, corpus callosum radial thickness measurements, thickness graph, GM and WM segmentation..... 40

Figure 3.26. Patient 26- Sagittal T1, corpus callosum radial thickness measurements, thickness graph, GM and WM segmentation..... 40
Figure 3.27. Patient 27- Sagittal T1, corpus callosum radial thickness measurements, thickness graph, GM and WM segmentation..... 40
Figure 3.28. Patient 28- Sagittal T1, corpus callosum radial thickness measurements, thickness graph, GM and WM segmentation..... 40
Figure 3.29. Patient 29- Sagittal T1, corpus callosum radial thickness measurements, thickness graph, GM and WM segmentation..... 41
Figure 3.30. Patient 30- Sagittal T1, corpus callosum radial thickness measurements, thickness graph, GM and WM segmentation..... 41
Figure 3.31. Patient 31- Sagittal T1, corpus callosum radial thickness measurements, thickness graph, GM and WM segmentation..... 41
Figure 3.32. Patient 32- Sagittal T1, corpus callosum radial thickness measurements, thickness graph, GM and WM segmentation..... 41
Figure 3.33. Patient 33- Sagittal T1, corpus callosum radial thickness measurements, thickness graph, GM and WM segmentation..... 42
Figures 3.34 a and b: Graphic representation of (a) Individual patients and (b) controls mean corpus callosum thickness in mm (blue diamonds) vs. age in months (red blocks). 46
Figure 3.35 a – f: Box and whisker plots comparing mean values of corpus callosum thickness between patients and controls 47
Figure 3.36 a - f: Box and whisker plots comparing maximum values of regional corpus callosum thickness (a) whole corpus callosum, (b) prefrontal corpus callosum, (c) premotor corpus callosum, (d) motor corpus callosum, (e) sensory corpus callosum and (f) visual corpus callosum between patients and controls 49

Figure 3.37. (a) Patients and (b) controls mean corpus callosum length in mm (red blocks) vs. age in months (blue diamonds) 50

List of Tables

Table 1.1. A summary of the main components of the current research as compartmentalised for publication..... 5

Table 3.1 a and b: Whole and segmental mean corpus callosum thickness (after averaging all the measurements obtained for a particular segment) across (a) controls and (b) patients 31

Table 3.2 a and b: Whole and segmental maximum corpus callosum thickness and corpus callosum length across (a) controls and (b) patients 32

Table 3.3. Brain volumes (TBV, GMV and WMV) (in ml) for (a) controls and (b) patients . 33

Table 3.4. Summary Statistics for Griffiths Mental Development Score (GMDS) : General Quotient (GQ) and Sub Scores (Locomotor and Language)(Patients Only)..... 43

Table 3.5. Summary Statistics of clinical and laboratory parameters (Patients only) 44

Table 3.6. Correlation of corpus callosum measurements with age 45

Table 3.7 (a) means and (b) maximums: t-test results for normally distributed variables [Overall corpus callosum, Prefrontal corpus callosum, Premotor corpus callosum, Visual corpus callosum, Sensory corpus callosum (max only), total brain volume, white matter volume and grey matter volume]..... 52

Table 3.8. Wilcoxon test for non-normally distributed variables (Motor corpus callosum, Sensory corpus callosum)..... 54

Table 3.9. Correlation of corpus callosum thickness (mean and maximum) and corpus callosum length with brain volume measurements (TBV, WMV, GMV) 55

Table 3.10. Correlation of corpus callosum thickness (mean and maximum) with Griffiths Mental Development Scores..... 57

Table 3.11. Correlation of CC thickness (mean and maximum) with clinical / laboratory parameters 58

Table 3.12. Correlation of corpus callosum thickness (mean and maximum) with laboratory parameters (nadir CD4, CD4 closest to scan) 59

Table 3.13. Correlation of corpus callosum length and clinical / laboratory parameters (patients only) 60

Table 3.14. Correlation of brain volumes with clinical parameters (GMDS and microcephaly) and laboratory parameters (time on HAART and CD4) 61

Table 3.15. Inter-class correlation and standard error of measurement of two different operators generating measurements using the software 62

Table 4.1. Comparison of research of corpus callosum thinning spanning 2007 – 2014 ... 72

List of Abbreviations

ADHD	Attention Deficit Hyperactivity Disorder
AIDS	Acquired Immune Deficiency Syndrome
ART	Anti-Retroviral Therapy
AZT	Azidothymidine (Zidovudine)
cART	Combined Anti-Retroviral Therapy
CC	Corpus Callosum
CHER	Children with HIV Early antiRetroviral trial
CNS	Central Nervous System
DTI	Diffusion Tensor Imaging
FAS	Foetal Alcohol Syndrome
FA	Fractional Anisotropy
GMV	Grey Matter Volume
GMDS	Griffiths Mental Development Scale/Score
GQ	Griffiths General Quotient
HAART	Highly Active Antiretroviral Therapy
HIV	Human Immunodeficiency Virus
HIVE	HIV Encephalopathy
ICC	Intra-class Correlation Coefficient
IRIS	Immune Reconstitution Inflammatory Syndrome
IQ	Intelligence Quotient
MR	Magnetic Resonance
MRI	Magnetic Resonance Imaging
SD	Standard Deviation
SEM	Standard Error of Measurement
SPM	Statistical Parametric Mapping
TBV	Total Brain Volume
WMV	White Matter Volume

1. Introduction

1.1. Hypothesis

Corpus callosum thickness (overall and segmental means and maximums in mm), as measured on sagittal T1-weighted MRI, will correlate with brain volume and developmental scores in children with HIV-related brain disease.

1.2. Justification of the research question

Neuroimaging with Magnetic Resonance Imaging (MRI) is proving to be a valuable diagnostic method for the assessment of central nervous system (CNS) involvement in patients with HIV and is also useful for monitoring disease progression and response to treatment by evaluating the degree of cerebral atrophy (1). Atrophy occurs in up to 78% of children with HIV-related encephalopathy (2).

Since most radiological interpretation is subjective and because the evaluation of atrophy (which may be mild or changing in response to disease or therapy) may be difficult, an objective measure of atrophy is desirable. Quantitative evaluation of the degree of white matter disease using volumetric assessment of white matter is possible (3) but is not practical for clinical use as it involves elaborate segmentation techniques using specific software. This is labour intensive and requires software expertise (4, 5). The mid-sagittal image is a routine brain MR image generated mainly for evaluating cerebral midline anatomy. A linear corpus callosum (CC) thickness measurement can be performed quickly using available measurement cursors on MRI scanners, a procedure familiar to

radiologists. If such a linear measure is proven to correlate with cerebral volume loss, it could be used as a surrogate marker of brain atrophy. This would not only improve detection of atrophy, but also allow determination of severity and monitoring of disease on follow-up studies in the clinical environment.

1.3. Study Aim

This study aims to determine whether the thickness of the CC (as viewed on mid-sagittal MRI) can be used as a surrogate marker of brain volume in children with HIV-related brain disease and to determine whether thickness at particular locations correlates with mental development scores and laboratory / clinical markers of immunity.

1.4. Study Objectives

- To determine the thickness of the CC on sagittal MRI in children with HIV-related brain disease and in appropriate controls, using a customised software tool.
- To determine the total brain volume (TBV), segmented grey matter volume (GMV) and segmented white matter volume (WMV) in children with HIV-related brain disease and in appropriate controls, using a validated publically available segmentation software package.
- To correlate CC thickness with brain volume in children with HIV-related brain disease and in appropriate controls.
- To compare CC thickness and brain volume in children with HIV-related brain disease against the values obtained for their controls and to determine which segments of the CC are most affected by HIV

- To correlate CC thickness (overall and segmental means and maximums) with mental development scores in children with HIV-related brain disease.
- To correlate CC thickness (overall and segmental means and maximums) with laboratory indicators of immunosuppression (CD4) in children with HIV-related brain disease.
- To correlate brain volume (TBV, GMV, WMV) with mental development scores in children with HIV-related brain disease.
- To correlate brain volume (TBV, GMV, WMV) with laboratory indicators of immunosuppression (CD4) in children with HIV-related brain disease.
- To determine inter-observer agreement for the determination of CC thickness using the customised software tool.

1.5. Preview and Organisation of the Thesis

The thesis will follow a standardised format regulated by the University of the Witwatersrand style guide.

This includes an 'Introductory Chapter' comprising: a literature review which provides information on: the corpus callosum, including definition, development, functional segments, thickness, causes of thinning and clinical correlates of thinning; central nervous system imaging in children with HIV, brain volume in HIV, and volumetric measures of the brain; HIV effects on the corpus callosum and these variables in the era of highly active anti-retroviral therapy (HAART) and includes statements relating to the source of data, methods of procedures and treatment of findings.

Next follow the ‘Central Chapters’, which provide detailed methodology and results of the current research.

Lastly, the thesis provides ‘Concluding Chapters’, encompassing a discussion of the results, a detailed description of limitations, a conclusion and recommendations. The document terminates with appendices and a reference list.

Five publications have arisen out of this research, ranging from the planning of the study, to the development of the techniques for measurement, to the literature review of the corpus callosum thickness, to the results. Related to the planning, a paper was written from the same patient population which reflects the author’s interest in the white matter pathology seen in children with HIV-related brain disease. The second paper defines the method developed for semi-automated measurement of the corpus callosum thickness and is a technical report. The third paper reflects the literature review relating to thinning of the corpus callosum in children in the form of a review article. The fourth and fifth papers present the objectives and results of the current research. The components of this research and publications arising there from are summarised in Table 1.1 below.

Table 1.1. A summary of the main components of the current research as compartmentalised for publication

	Published		Published		Progress, Unpublished and Pipeline
1	**Background - Clinical Utility of MRI:** Ackermann C, **Andronikou S**, Laughton B, Kidd M, Dobbels E, Innes S, et al. White matter signal abnormalities in children with suspected HIV-related neurologic disease on early combination antiretroviral therapy. Pediatr Infect Dis J. 2014;33:e207-212. (50: 50 contribution with Dr Ackerman who is first author – letter of contribution is attached as appendix B)	**3**	**Serving as literature review:** **Andronikou S**, Pillay T, Gabuza L, Mahomed N, Naidoo J, Hlabangana L T, et al. Corpus callosum thickness in children: an MR pattern-recognition approach on the midsagittal image. Pediatr Radiol. 2015;45:258-272.	**6**	**Advanced MRI Techniques:** Fractional anisotropy of the white matter derived from DTI in HIV infected children and correlation with clinical and laboratory markers (Dr Ackerman is first author and I am her supervisor for her PhD on this topic).
2	**Methods: Technical report** **Andronikou S**, Spottiswoode B, S., Tomazos N. A semi-automated method for measuring thickness and white matter integrity of the corpus callosum. South African Journal of Radiology. 2012;16:130-133.	**4**	**Serving as results:** **Andronikou S**, Ackermann C, Laughton B, Cotton M, Tomazos N, Spottiswoode B, et al. Correlating brain volume and callosal thickness with clinical and laboratory indicators of disease severity in children with HIV-related brain disease. Childs Nerv Syst. 2014;30:1549-1557.	**7**	**Inter-observer agreement testing:** Reliability of a semi-automated tool for measuring corpus callosum thickness: an inter-reader comparison of two operators (This is included in the research but is unpublished.)
		5	**Serving as results:** **Andronikou S**, Ackermann C, Laughton B, Cotton M, Tomazos N, Spottiswoode B, et al. Corpus callosum thickness on mid-sagittal MRI as a marker of brain volume: a pilot study in children with HIV-related brain disease and controls. Pediatr Radiol. 2015;45:1016-1025.	**8**	**Possible additional measurements would really constitute new work:** - Basal ganglia linear measures correlated with development and measures of immunity - Ventricular measures correlated against brain volume (Similar work done previously for tuberculosis.)

1.6. Literature Review

1.6.1 Definition and function of the corpus callosum

The CC is the largest white matter (i.e. myelinated axonal pathway) structure and largest commissure of the brain connecting the two cerebral hemispheres in the human (6-10). It is the main structure for information transfer between the cerebral hemispheres (8) and is thought to transfer sensory and higher process information for integrating the activities of the two hemispheres (6, 9). The CC reportedly unifies sensory fields, organises bimanual output, aids in memory storage and retrieval, allocates attention and arousal, facilitates language and auditory processes and may also play a role in consciousness, intelligence, learning, executive functioning and social cognition (6, 8).

1.6.2 Development and variability of the corpus callosum

The CC begins to develop at around eight weeks after conception, with the maximum number of axons crossing the CC in utero and an adult morphology achieved at around 115 days of gestation (6, 8). There is a fixed number of fibres after birth (11) but postnatal changes occur and continue during childhood and adulthood via myelination, re-organisation and pruning of these fibres (6, 8, 10, 11). The maximum CC size is achieved between 6 – 15 years of age (11). There is, however, significant individual variation in CC morphology (6). The anterior CC reaches its maximum size earlier than the middle and posterior portions (12). Most variability in size and shape is found more posteriorly at the isthmus and splenium (13). In addition, most maturation changes across the age spectrum involve this posterior portion of the CC (6). This is in part due to a difference in the

histology, with smaller unmyelinated fibres anterior (genu) and large myelinated fibres in the middle (isthmus) and posterior parts (splenium) (10, 12). This is also reflected in diffusion tensor imaging (DTI) studies, which demonstrate higher anisotropy posteriorly than anteriorly (a measure of fibre integrity) (12, 13). The splenium can be circular or long and with or without an obvious isthmus (13). The most recent morphologic data obtained by Garel and colleagues from 622 children using MRI, demonstrate that there is rapid growth until three years of age, after which stabilisation of the isthmus-splenial thickness ratio occurs (considered indicative of CC modelling) (10). They also demonstrated a progressive increase in length of the CC throughout childhood and showed no significant differences in length or thickness between boys and girls (10).

1.6.3 Functional units of the corpus callosum

General descriptions of the CC segments relate the splenium topographically to occipital white matter and the body to the pre- and post-central gyri (14). Slightly more detailed descriptions indicate that the posterior CC body connects the primary motor/premotor and parietal association areas, the isthmus connects primary sensory, primary motor, posterior parietal and superior temporal areas and that the anterior splenium connects the posterior parietal and inferior temporal areas (7). DTI fibre tracking techniques (which are methods of demonstrating white matter fibre anatomy using MRI) have been used to segment the CC 'into bands that correspond to functional units' rather than the traditional segmentation relying on the shape of the CC (15). Five vertical functionally related segments have been defined and their fractional anisotropy (FA) measured:

1. Anterior 1/6th of the CC is related to the **prefrontal cortex**

2. The segment between the anterior 1/6th and the midpoint of the CC is related to the **premotor and supplementary motor cortices**
3. The portion between the midpoint and posterior third of the CC is related to the **primary motor cortex**
4. The portion between the posterior third and posterior quarter is related to the **primary sensory cortex**
5. The posterior quarter relates to the **parietal, temporal and occipital cortices** (12, 14)

Even more specifically, the visual cortex ('cortex dorsal to the calcarine fissure') relates to the anterior half of the splenium; the 'cortex ventral to the calcarine fissure' relates to the 'anterior – inferior edge of the splenium' and the 'occipital pole and lateral occipital regions' relate to the part anterior to the centre of the splenium (15). The splenium has the highest measured FA at 0.8, regardless of age, indicating that it is the most organised area and contains the most intact axons, while the mid CC (premotor, motor and sensory) has the lowest measured FA (0.2 – 0.4) (14). Overall, these findings can be interpreted to reflect that: (a) the anterior portion of the CC is the least likely to change with development of the brain and thus can be used for reference and (b) the posterior portion of the CC (in particular the splenium and isthmus which represent a concentrated group of axons) reflects the development of the parietal, temporal and occipital lobes and has the highest variability.

Some researchers do not use subsections in their analyses. Northan and colleagues, who correlated intelligence quotient (IQ) and CC morphology, did not use subsections because total cross-sectional area and subsection areas do not affect IQ differently (16). They did

indicate, however, that motor and visuo-motor coordination correlates strongly with specific section morphology of the CC (16).

1.6.4 Corpus callosum thickness

The anterior portions of the CC change the least with age and vary the least between humans. This portion of the CC can be used as a reference point for comparing the thickness and FA of the posterior portions (13). At three months of postnatal age, the mid-point of the CC thickens as the connections between the pre- and post-central gyri (motor and sensory) myelinate (6). At 4-6 months, the splenium thickens as areas of visual association myelinate for binocular vision and visual accommodation (6). At pre-school age (5-6 years), the anterior CC (rostrum and genu) reaches adult thickness (6).

The midcallosal area is reported to be 'an indicator of the total number of small diameter' fibres in the CC (7). It is further reported that thickness of the CC reflects either the number of fibres or the degree of myelination of the CC (7, 17). Thinning of the CC has been determined by visual inspection in clinical practice by using midsagittal images on ultrasound and MRI. An example of this in paediatric practice is for evaluating dysmyelinating or demyelinating disorders and perinatal trauma with hypoxia (9, 10).

The CC may also be secondarily affected as a result of white matter fibre loss (18). Degeneration of commissural tracts secondary to peripheral white matter (WM) lesions shows prominent changes in the body of the CC, which correlate with the clinical assessment of cognition and motor control (19). Eighty percent of children with peri-ventricular leukomalacia have dilated ventricles in response to white matter volume

(WMV) reduction and there is thinning of the CC in 50% of these (18). Imaging studies have therefore used the CC as a surrogate marker for overall WM atrophy (13).

It is also hypothesised that a thicker CC indicates an increased number of fibres or greater myelination and therefore results in better cognitive performance through a number of mechanisms, including involvement of the appropriate hemisphere, increasing 'processing units by involving both hemispheres and allowing rapid co-ordinated use of processing units depending on specific tasks' (7). Garel and colleagues have recently made available normal values of CC thickness for children aged 1 day to 15 years of age (10).

1.6.5 Correlating corpus callosum size with disease and performance

CC thickness may relate to cognitive and non-cognitive functions such as motor or sensory functions (20). A larger CC size (especially posterior) is 'associated with better motor performance in children born with very low birth weight when measured at eight years of age' (18). One study showed that adolescent boys born pre-term who had low verbal IQ and poor verbal fluency had small mid and posterior CC areas on mid-sagittal imaging (21), while another study showed correlation of CC area with overall IQ (16).

Thinning of the CC has been reported to occur in a localised pattern with trauma (22, 23), surgery (23) [Figure 1.1], infarction (23, 24), metabolic diseases (25), hypoglycaemia (posterior) (23) and hypoxic ischaemic encephalopathy (predominantly posterior) (25) [Figure 1.2]. Generalised thinning of the CC has been reported to occur with failed or abnormal myelination (7, 17, 26) and diffuse injury from hypoxic ischaemic

encephalopathy (18, 24) [Figure 1.3], HIV (4, 27) and hydrocephalus (28).

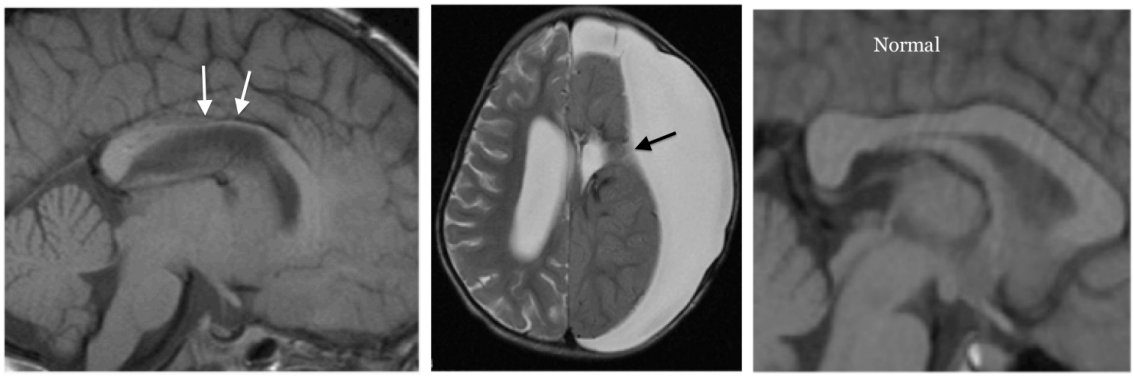


Figure 1.1. Sagittal T1 MRI image of central corpus callosum thinning (white arrows) corresponding to unilateral brain loss after excision of a left-sided tumour (black arrow) on T2, with a comparison sagittal T1 weighted image showing thickness of the corpus callosum in a normal child (Normal)

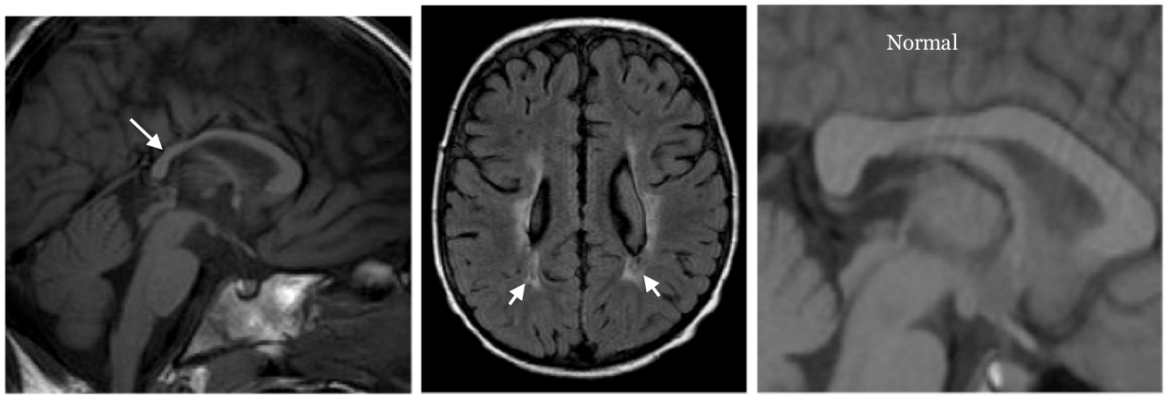


Figure 1.2. Sagittal T1 weighted image showing predominantly posterior corpus callosum thinning (long arrow) corresponding to predominantly posterior peri-ventricular leukomalacia (short arrows) on FLAIR after a perinatal hypoxic insult, with a comparison sagittal T1 weighted image showing thickness of the corpus callosum in a normal child (Normal)

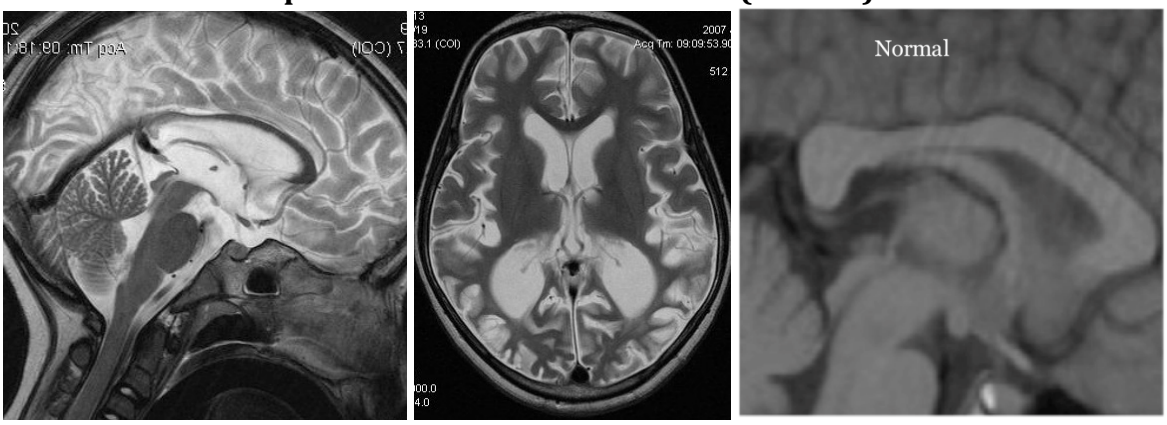


Figure 1.3. Sagittal T2 showing generalised corpus callosum thinning related to global white matter volume loss after a global hypoxic event at birth as seen on axcial T2, with a comparison sagittal T1 weighted image showing thickness of the corpus callosum in a normal child (Normal)

1.6.6 CNS imaging in children with HIV and its effects on brain volume

HIV encephalopathy (HIVE) is an AIDS-defining event (2), which occurs in vertically infected infants and children. There is loss of brain growth, motor abnormalities occur and cognitive dysfunction is identified (29, 30). A sensitive predictive marker of encephalopathy is critical (27, 31) because early additional neuroprotective treatment may preserve brain integrity, slow deterioration or partially improve symptoms (27, 29, 32). There is current evidence that suggests that intensive anti-retroviral therapy may halt or even reverse encephalopathy, leading to improved neurocognitive outcome and survival in children with HIV dementia (31, 33, 34).

The most common pathological feature of HIVE is diffuse WM involvement, especially in the advanced stage of the disease (35). HIV leukoencephalopathy is 'a triad of diffuse myelin loss, astroglial proliferation, and infiltration by mono- and multi-nucleated macrophages' (36). Children have distinct patterns of CNS involvement in HIV infection, which differ from adults, and have been defined by States and colleagues for children less than two years of age (37). They have not, however, been defined for older children (38). The aim of management is to rapidly identify infants at risk of CNS 'disease progression and institute effective treatment that can halt devastating effects of HIV on the developing brain' (30). MRI may have a role to play in the early detection of HIVE and in the prediction of developmental outcome without and with treatment (36).

Neuroimaging has been utilised to follow the course of HIV-infected children with neuro-psychological problems (39). It has three roles in evaluating the HIV-infected child: (a) it is a screening tool for detection of cerebral atrophy or early signs of encephalopathy; (b) it

is a primary diagnostic tool for detection of complications such as lymphoma, stroke, and opportunistic infections; and (c) it is useful for follow-up after initiation of anti-retroviral therapy to determine response to treatment (1). MRI screening, therefore, has been suggested for high-risk children and is advisable when evidence of neurological symptoms or neurocognitive dysfunction is noted (40).

The most common imaging findings in children with HIVE are basal ganglia calcification and atrophy (2, 41, 42). In one study (conducted in 1998 using CT and MRI), every child with a diagnosis of encephalopathy had a positive neuroimaging finding – either atrophy or basal ganglia calcifications (42). Cerebral atrophy and ventriculomegaly were present in 68 and 78% of HIV infected children with symptomatic disease, respectively (2). More recently white matter signal abnormality has also been demonstrated on MRI in HIV-infected children (43).

Studies in adults with AIDS have measured atrophy in the basal ganglia (specifically the corpus striatum), parietal grey matter, peri-central regions, cingulum, and white matter, including the CC (4, 5). Atrophy of the brain in adults with HIV has been shown to be associated with low CD4 counts (4, 5) and with neuropsychological impairment (5). Chiang and colleagues believe that white matter atrophy and Wallerian degeneration may be secondary to cortical thinning in adults with HIV (5).

1.6.7 MRI Volumetric techniques

Standard structural MRI lacks the sensitivity to detect subtle volume and white matter abnormalities in HIV-related brain disease (5). Volumetric techniques are therefore

valuable for identifying subtler *in vivo* morphometric changes in the brain (3). 'Manual delineation by trained experts is the gold standard' for determining the volume of structures, (3) but most researchers and clinicians use popular Statistical Parametric Mapping [SPM: Wellcome Trust Centre for Neuroimaging UK], which is well published, automated and therefore less labour intensive. This technique 'employs an atlas based segmentation approach to generate individualised anatomical labelled map for a spatially normalised image, based on an atlas of manually traced reference scans' (3). Ances and colleagues report that brain volume assessment may be a robust way of quantifying brain integrity in adults with HIV (27).

'Automated' techniques are preferred to manual measurements (which are extremely labour intensive and time consuming), but are not automated enough for clinical use (4, 5). This drives the ongoing search for clinically useful and quick surrogate methods reflecting clinical parameters (4).

1.6.8 Corpus callosum in HIV

The areas of the brain most affected in HIV are those close to the ventricles, because there is 'easier viral penetration by HIV-infected mononuclear cells trafficking from cerebrospinal fluid into brain', and a higher concentration of HIV toxins in these cells (4, 27). Consequently, the highest brain concentrations of HIV are found in the caudate nuclei and CC (4, 27). Ances and colleagues noted that decreases in brain volume in HIV-infected adults included a decrease in volume of the CC (27). Chiang and Dewey have also shown changes in CC volume in patients with HIV (3, 5).

Thompson and colleagues believe that 'white matter deficits may be easier to detect at the midline than globally' (4). Their findings support the 'use of CC thickness as an MRI marker of white matter integrity' in adults with AIDS (4). We believe that overall thickness and the thickness of the various functional segments of the CC can be used to assess white matter volume loss and correlate with clinically assessed developmental scores in children with HIV. Currently, because there is no available technique for measuring brain volume rapidly in the clinical setting, linear thickness of the CC may represent a rapid surrogate measure. This is done easily, by simply placing the measurement cursors available on all MRI scanners, without a need for computerised software such as the customised tool described and used for this research below.

There are no previous studies of CC thickness as a surrogate marker of white matter volume loss in children with HIV, internationally or locally, and we believe this to be the first study of its kind. Precedent for the use of CC thickness in children exists in various studies, including: the evaluation of peri-ventricular leukomalacia (there was thinning of the CC) (18); a study using the CC as a surrogate marker for overall WM atrophy (13); a study correlating CC thickness on mid-sagittal imaging with motor performance (18) and a study correlating CC thickness with verbal IQ and verbal fluency (21). There are, however, previous publications using CC thickness in HIV-infected adults. Thompson and colleagues recognised the use of surrogate markers of disease burden in HIV-infected adults and they showed significant thinning of the CC involving predominantly the anterior three sectors (up to 25 % thinner than controls). This thinning of the CC midbody and rostrum showed significant correlation with CD4 levels (4), which is explained by the fact that

'severe immune deficiency' (low CD4 counts) results in greater HIV replication which in turn results in HIV infection of the brain (44).

1.6.9 Corpus callosum thickness and brain volume in HIV in the HAART era

Although HAART has resulted in an approximately 50% decrease in HIV-related dementia in adults, HIV encephalitis and other cognitive disorders are now more prevalent (4). Thompson and colleagues suggested that HAART might not in fact protect the brain from HIV-related brain degeneration, as traditional anti-retroviral drugs 'have difficulty crossing the blood-brain-barrier' (4). In 2007, HIV encephalopathy was still identified in 25 % of AIDS-related adult autopsies (5). Numerous studies show that cortical atrophy continues in the HAART era (44). Becker and colleagues showed significant atrophy of the corpus striatum in adults with HIV, who were being treated with HAART, which was related to the length of time they had been diagnosed as sero-positive (45). These authors suggested that either atrophy is a chronic subclinical process occurring despite treatment, or the extent of the initial insult dictates the extent of the atrophy (45). Chiang and colleagues concur with their findings, showing no difference in the degree of brain atrophy between adults on HAART and those not on HAART. They postulated that HAART may not save the brain tissue but it still has a role in improving neurocognitive function (5). More recently, Cohen and colleagues also showed that HIV-infected patients on HAART are vulnerable to brain disturbances and that specific brain regions are more susceptible to volume loss than others (44).

1.6.10 How the current research has arisen from the failures / inadequacies of previous work

Previous imaging research related to brain volumes, CC thickness and their relationship to clinical markers of disease severity and outcome in HIV has been predominantly in adults. These findings cannot be translated directly to children. This is because children acquire their disease differently, are infected for different periods of time, present different morphologies in the brain depending on age and development, and respond differently to HIV and its treatment. Different imaging tests specific to children are therefore needed to determine the outcome of disease on cognition and functioning.

Previous paediatric research relating to the CC has not addressed the effects of HIV infection, but rather has concentrated on the effect of hypoxic ischaemic encephalopathy. Previous research regarding the CC in adults has predominantly concentrated on volumetric assessment of this structure but has not as yet offered a clinically useful linear measure of disease for radiologists to use in clinical practice. Volumetric measures are labour intensive and require expertise in a field very different from clinical radiology. In addition, morphological brain changes in children have not previously been correlated with clinical parameters important for determining severity and progress of HIV or with mental development tests. There is limited research correlating brain morphology with clinical parameters in the HAART era where HIV infection represents chronic effects on the brain and where drug toxicity may play a role.

2. Materials and Methods

2.1. Study Design

This is a nested, cross-sectional retrospective study of children diagnosed with HIV-related brain disease. The larger study, in which this is nested, is designed to test MRI detection of white matter pathology in children infected with HIV using both standard and advanced quantitative MRI sequences.

2.2. Study Setting

The measurements were performed on digitally recorded MRI scans. This patient material was derived from the paediatric population of the Western Cape presenting to the Tygerberg Hospital and University of Stellenbosch Radiology department (for imaging). The patient material was used with permission from the leader (Prof. M Cotton) of the larger study in which this study is nested, the Children with HIV Early Antiretroviral (CHER) trial, which contributed all of the children referred for MRI.

2.3. Study Population

The study was performed over two and a half years at Tygerberg Children's Hospital, a referral hospital in Cape Town, South Africa. Children included were those who were referred for MR neuroimaging by their infectious disease clinicians because of suspicion of HIV-related neurological disease (poor head growth, long tract signs or neurodevelopmental delay).

Mothers were on the prevention of mother-to child transmission (PMTCT) program, which included Zidovudine (Azidothymidine, AZT) antenatally from 32 weeks and a single dose of Nevirapine at delivery to the mother as well as a single dose of Nevirapine and seven days of AZT to the infant. Mothers with a CD4 count below 250 cells per mm^3, received cART (combined anti-retroviral therapy) antenatally.

Participants were regularly followed up with clinical assessments monthly, which included neurological examination and head growth monitoring. Clinicians performed neurodevelopmental screening assessments every 6 months and a developmental paediatrician undertook a comprehensive developmental assessment using the Griffiths Mental Development Scale (GMDS) (46) at 12, 18, 30 and 42 months.

Baseline data, including clinical data and neurodevelopmental scores, were obtained from participants' medical records.

MRI scanning was performed at a tertiary referral centre on a Siemens Magnetom Symphony 1.5T (Erlangen, Germany). Sequences included axial Spin Echo T2-weighted (T2 SE), axial Fluid Attenuation Inversion Recovery (FLAIR), sagittal T1-weighted Spin Echo (T1 SE), sagittal T2-weighted Spin Echo (T2 SE), diffusion weighted imaging (DWI), and a post gadolinium axial T1-weighted with a slice thickness of 5mm.

2.4. Sampling

Sample size was restricted by available MRI scans performed for the study in which the current study was nested.

2.5. Inclusion Criteria

All children (13 years old and under) presenting at one academic tertiary referral centre with clinical evidence of suspected HIV-related brain disease (impaired head growth, neurodevelopmental delay and long tract signs) and available MRI scans (over a two and a half year period when the larger study was performed) were included. The following were reasons for referral for neuroimaging:

1. Failure to attain or loss of developmental milestones or loss of intellectual ability.
2. Impaired brain growth based on head circumference measurements
3. Acquired symmetric motor deficits manifested by: pathological reflexes or abnormal tone.

Controls were obtained from any clinically indicated MRI scans reported as 'normal', matched for age and gender, at the same institution. These controls represent the same geographic population group and were scanned using the same MRI equipment. Reasons for referral of controls to MRI included 'headache' and 'sinusitis imaging'.

2.6. Exclusion Criteria

Patients were excluded if there was evidence of any of the following: previous opportunistic CNS infection, CNS neoplasm, neurological disease caused by factors other

than HIV, previous anoxic insults, persistent metabolic derangement, dysmorphic features. Patients were also excluded if MRI scans were unavailable, incomplete (sequences and planes) or inadequate (due to motion artefact, metallic artefact, etc.). Children with abnormal neurological assessments were excluded from the control group. In addition, patients and controls were excluded whenever the post processing measuring instruments did not result in adequate images / measurements.

2.7. Measurement Instruments

2.7.1 CC thickness measurement

A software program was developed 'in-house' (by: Bruce Spottiswoode, University of Cape Town) whereby MRI data can be imported into a custom tool written in MATLAB (The Mathworks Inc, Natick, MA). A description of this technical innovation was published in 2012 (47) and the method of deriving multiple automated thickness measurements of the CC is similar to a previously described method by Luders and colleagues (7), but was developed independently. The operator selects the midline sagittal position of a T1-weighted image (using the aqueduct of Sylvius as a landmark) via the customized tool. Dorsal and ventral CC contours are manually drawn on the mid-sagittal image using a point depositing system. This initiates an automated calculation of a contour midway between these manually drawn lines (referred to by some authors as the CC diameter (10)). The program is designed to then divide the midline contour into a pre-selected number of segments and perpendicular spokes are projected from each segment until they intersect with the dorsal and ventral contours (Figure 2.1 a). The number of segments is limited by the spatial resolution and a maximum of 40 segments was chosen for this application to ensure that each segment still consists of a contiguous strip of

voxels across the CC from the dorsal to the ventral contour. The system yields between 36 and 40 measures of 'thickness' (as opposed to the method of Luders and colleagues which produces 100 segments (7)) and automatically plots segment thickness as a function of distance along the midline CC contour (CC diameter) (Figure 2.1 b). This tool was validated on six normal adult volunteers and one patient with multiple sclerosis and proved successful in measuring and plotting CC midline thickness and fractional anisotropy (47). The current study utilised the customised measuring software for convenience to derive multiple computer-generated results. This study did not intend to promote the use of the software for deriving CC linear measures in clinical practice. The primary investigator determined the thickness measurements using the software and his results were used for correlations and comparisons. A second reader performed the same procedure on all patients and controls blinded to the primary reader's results, to determine inter-observer correlation.

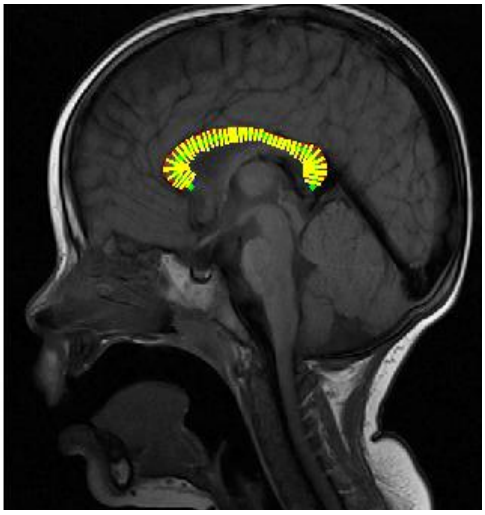
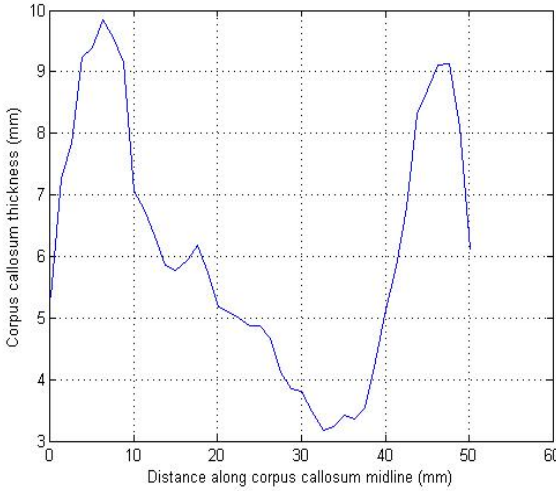
(a)  (b) 

Figure 2.1 a and b: corpus callosum thickness measurement: (a) Midline sagittal T1 weighted MRI indicating the 40 radial measurements of thickness produced by the custom-made semi-automated tool and (b) plotted along the length (diameter) of the corpus callosum automatically from start of the genu (at 0 mm) to the end of the splenium (at 50 mm).

2.7.2 Brain volume calculation

To calculate total brain volume (TBV), grey matter volume (GMV) and white matter volume (WMV), axial T2-weighted MRI scans of each patient were analyzed using MATLAB 7.3 (The MathWorks Inc, Natick, MA) and Statistical Parametric Mapping software (SPM5, Wellcome Department of Imaging Neurosciences, University College London) using voxel-based morphometric (VBM) analysis. This is a whole-brain technique for characterizing volume and tissue "concentration" differences in structural MRIs. The MRI scans were spatially normalised towards a template of normal MRI scans. The normal MRI template used in the current study is a template designed for children and released by the Imaging Research Center, Cincinnati Children's Hospital Medical Center, and is freely available on the Internet (https://irc.cchmc.org/software/cchips.php). The normalised images were then segmented into gray matter and white matter and the volumes of each were derived using the automated volume calculation, 'Easy Volume'.

2.8. Data

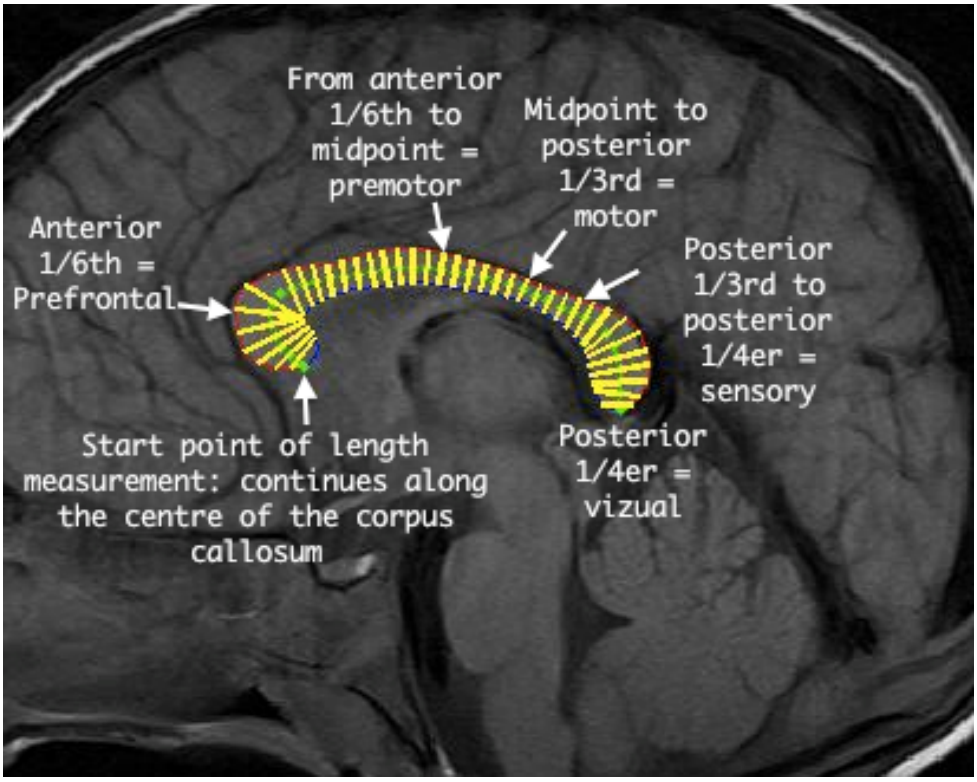
2.8.1 Overall mean and maximum CC thickness

This was determined in millimeters (mm) for each patient and each control using the full number of measurements produced.

2.8.2 Segmental CC mean and maximum thickness

These were determined for each segment for each patient and control according to segments described by Hofer et al (14), by including thickness of all measurements within each segment and generating a mean (Figure 2.2 a and b): the 'Prefrontal' segment (anterior $1/6^{th}$ – by dividing the full number of segments by 6); 'Premotor' segment (between anterior $1/6^{th}$ and the midpoint); 'Motor' segment (midpoint to posterior third - by dividing the full number of segments into 3); 'Sensory' segment (posterior third to posterior quarter by dividing the full number of segments into 4) and 'Language' / 'Visual' segment (posterior quarter).

(a)



(b)

Region	arc length (r	CC thickness (mm)	prefront 6	PreM 14	motor 6	sensory 4	viz 10
1	0,626138	6,250859624	6,250859624				
2	1,878415	7,547358241	7,547358241				
3	3,130691	8,537108492	8,537108492				
4	4,382968	9,324313413	9,324313413				
5	5,635244	9,628026145	9,628026145				
6	6,887521	9,704190095	9,704190095				
7	8,139797	9,355210288		9,35521			
8	9,392074	8,108219058		8,108219			
9	10,64435	6,912360471		6,91236			
10	11,89663	6,541855637		6,541856			
11	13,1489	6,087947621		6,087948			
12	14,40118	5,810549109		5,810549			
13	15,65346	5,853363865		5,853364			
14	16,90573	6,056208602		6,056209			
15	18,15801	5,956723476		5,956723			
16	19,41029	5,463444896		5,463445			
17	20,66256	5,147915027		5,147915			
18	21,91484	5,049311738		5,049312			
19	23,16712	4,928503876		4,928504			
20	24,41939	4,865479807		4,86548			
21	25,67167	4,762404278			4,762404		
22	26,92395	4,391828775			4,391829		
23	28,17622	3,991387783			3,991388		
24	29,4285	3,830040158			3,83004		
25	30,68077	3,644145323			3,644145		
26	31,93305	3,327857037			3,327857		
27	33,18533	3,203461541				3,203462	
28	34,4376	3,32939208				3,329392	
29	35,68988	3,39424195				3,394242	
30	36,94216	3,457849177				3,457849	
31	38,19443	3,925575669					3,925576
32	39,44671	4,71782068					4,717821
33	40,69899	5,478435478					5,478435
34	41,95126	6,310935239					6,310935
35	43,20354	7,551030442					7,55103
36	44,45582	8,507301039					8,507301
37	45,70809	8,913448342					8,913448
38	46,96037	9,124209724					9,12421
39	48,21265	8,616439382					8,616439
40	49,46492	7,109251039					7,109251
		244,7160046	50,99185601	86,13709	23,94766	13,38494	70,25445
		6,125	8,5	6,1	4	3,3	7

Figure 2.2 a and b: (a) Annotated midline sagittal MRI demonstrating the predefined corpus callosum segments and (b) calculation of mean thickness by inclusion of all measurements within a segment

2.8.3 CC length (from tip of rostrum midpoint to tip of splenium midpoint)

This was determined for each patient and control and a mean was determined for both groups.

2.8.4 Brain volumes

These were determined as TBV in milliliters (ml) by adding the calculated GMV and WMV for both the patients and controls. Mean TBV, GMV and WMV were also determined.

2.8.5 Griffiths Mental Development Scores (GMDS)

Clinicians performed neurodevelopmental screening assessments every six months and a developmental paediatrician undertook comprehensive developmental assessments using the Griffiths Mental Development Scale (GMDS) (46) at 12, 18, 30 and 42 months. We used the GMDS **performed closest to the time of the MRI scan.** Griffiths quotients were obtained from raw scores or age equivalents using the United Kingdom Norms with a mean of 100 and standard deviation of 15 (46, 48). Significant developmental delay was regarded as more than 2 standard deviations below the mean i.e. quotients lower than 70.

2.8.6 Clinical and laboratory data

Clinical and laboratory data for each of the patients were available from the larger study in which this study was nested and included CD4 level (cells per mm^3), nadir CD4 (the lowest CD4 recorded for the patient, excluding the baseline measure)(cells per mm^3), length on ART (in weeks) and viral load (lowest level of detection reported as <400 HIV RNA copies/mm^3 and patients were categorized as < or >400copies/mm^3)

2.9. Data Analysis

Data were captured on an Excel spread sheet and were summarised as mean and standard deviations for continuous variables [age, CC thickness (mm), CC length (mm), TBV, GMV, WMV (ml), developmental scores, CD4 (cells/mm^3), nadir CD4 (cells/mm^3), length on ART (days), viral load (copies/mm^3)] where normality applied, and median and interquartile range when data were not normally distributed. Categorical variables [patients / controls; males / females] were recorded as frequencies and percentages.

Comparisons between patients and controls was performed using an independent t-test and a Man-Whitney Wilcoxon test (for continuous non-normally distributed variables) with regard to overall mean CC thickness, mean segmental thicknesses and WMV.

The Pearson correlation was used for normally distributed values and Spearman correlation for non-normally distributed values. Overall mean and maximum thickness of the CC as well as segmental mean and maximum thickness were correlated with brain volumes (TBV, GMV and WMV) for both patients and controls. Overall mean and maximum CC thickness and mean and maximum segmental thickness as well as brain volumes were correlated with general mental development scores and sub-scores (locomotor and language) as well as laboratory data in patients.

Uni- and multi-variate regression analyses were performed to predict brain volume (ml) and outcome score using the presence of HIV encephalopathy, CC thickness, age and gender as explanatory variables. Differences were considered significant if $p < 0.05$.

Inter-observer agreement between the two independent operators' generation of a mean of each CC segment and the overall mean thickness of the CC, was tested using a two-way

agreement model to determine the intra-class correlation coefficient (ICC) and a standard error of measurement (SEM).

2.10. Ethical Issues

MRI studies were indicated and performed for clinical reasons. No additional imaging was performed solely for the purposes of this research. The primary investigator of the larger study (in which the current research was nested) received ethical clearance from the University of Stellenbosch Ethics Committee (N07/09/208*/* and the current research, was approved by the University of Witwatersrand Human Research Ethics Committee (M110802) (Appendix I).

3. Results

Of a total of 48 patients and 16 controls included, only 33 patients and 11 controls remained after applying the exclusion criteria. Four patients were excluded because imaging was lost and an additional 11 patients and 5 controls were excluded because of motion artefact, which precluded adequate determination of volumes. Patients' ages ranged from 7 - 49 months (median 31 months; mean 30 months) and there were 16 boys and 17 girls. Controls ranged in age from 13 – 48 months (median 34 months; mean 32 months) and there were 6 boys and 5 girls.

3.1. General results of corpus callosum thickness, corpus callosum length and brain volume

Whole CC thickness and segmental CC thicknesses of patients (a) and controls (b) are summarised in Tables 3.1 (mean values) and 3.2 (maximum values). Brain volumes are summarised for patients (a) and controls (b) in Table 3.3. Individual pictorial and graphic representations of the CC thickness against length, as well as volume segmentation are presented in Figures 3.1 to 3.33 for patients 1 to 33.

Table 3.1 a and b: Whole and segmental mean corpus callosum thickness (after averaging all the measurements obtained for a particular segment) across (a) controls and (b) patients

Variable	N	Min	Max	Median	25th Percentile	75 Percentile	Mean	SD
(a) Controls								
Whole CC (mean)	11	3.7	7.6	6	5.3	6.2	5.7	1.0
Prefrontal CC (mean)	11	5.2	10.4	7.5	6.3	8.5	7.4	1.5
Premotor CC (mean)	11	3.4	7.4	5.6	5.3	6.1	5.5	1.2
Motor CC (mean)	11	2.7	6.2	4	3.8	4.8	4.3	1.0
Sensory CC (mean)	11	2.3	5.3	3.5	3	4.5	3.6	0.9
Visual CC (mean)	11	3.7	8.3	7	6.1	7.4	6.7	1.3
(b) Patients								
Whole CC (mean)	33	3.9	6.9	5.5	5.1	5.9	5.5	0.6
Prefrontal CC (mean)	33	4.8	10.5	7.2	6.8	7.8	7.3	1.1
Premotor CC (mean)	33	4.4	7.3	5.5	5	5.9	5.5	0.7
Motor CC (mean)	33	2.6	6.5	4.1	3.6	4.3	4.1	0.7
Sensory CC (mean)	33	2.2	5.1	3.2	2.6	4	3.3	0.8
Visual CC	33	3.5	8.5	6.2	5.6	7	6.2	1.2

Table 3.2 a and b: Whole and segmental maximum corpus callosum thickness and corpus callosum length across (a) controls and (b) patients

Variable	N	Min	Max	Median	25th Percentile	75 Percentile	Mean	SD
(a) Controls								
CC length	11	41.1	50.7	46.6	44.7	49.5	46.7	2.8
Whole CC (max)	11	6.3	11.6	9.4	8.4	10.4	9.4	1.6
Prefrontal CC (max)	11	6.3	11.6	9	7.4	10.3	9	1.7
Premotor CC (max)	11	4.8	10	7.9	6.5	9	7.6	1.7
Motor CC (max)	11	3.3	6.8	4.6	4.4	5.2	4.9	1.1
Sensory CC (max)	11	2.7	6	4	3.3	4.8	4.1	1
Visual CC (max)	11	4.6	10.5	8.8	8	9.6	8.6	1.6
(b) Patients								
CC length	33	41.3	54.7	48.3	47.4	50.3	48.9	2.7
Whole CC (max)	33	6.6	11.6	9.3	8.3	10.2	9.3	1.2
Prefrontal CC (max)	33	6.3	11.5	8.6	7.5	9.7	8.7	1.4
Premotor CC (max)	33	5.9	10.4	7.3	6.9	7.9	7.5	1
Motor CC (max)	33	3.5	6.9	4.6	4.4	5.1	4.7	0.7
Sensory CC (max)	33	2.4	5.4	3.7	3.1	4.5	3.7	0.9
Visual CC (max)	33	4.6	11.6	8.2	7.8	9.3	8.4	1.4

Table 3.3. Brain volumes (TBV, GMV and WMV) (in ml) for (a) controls and (b) patients

Variable	N	Minimum	Maximum	Median	25th Percentile	75 Percentile	Mean	SD.
(a) Controls								
GMV	11	500	857	628	589	735	647	107
WMV	11	269	423	335	273	360	327	52
TBV	11	774	1280	975	862	1083	974	148
(b) Patients								
GMV	33	500	800	632	589	679	632	76
WMV	33	257	430	369	327	382	355	45
TBV	33	820	1184	1009	901	1047	987	93

Key: GMV = grey matter volume; WMV = white matter volume; TBV = total brain volume

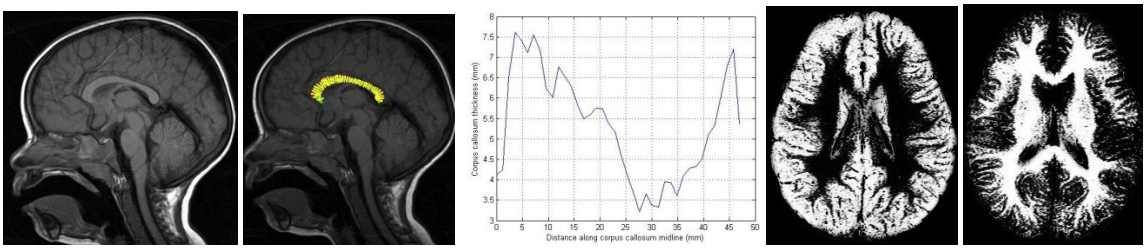


Figure 3.1. Patient 1- Sagittal T1, corpus callosum radial thickness measurements, thickness graph, GM and WM segmentation

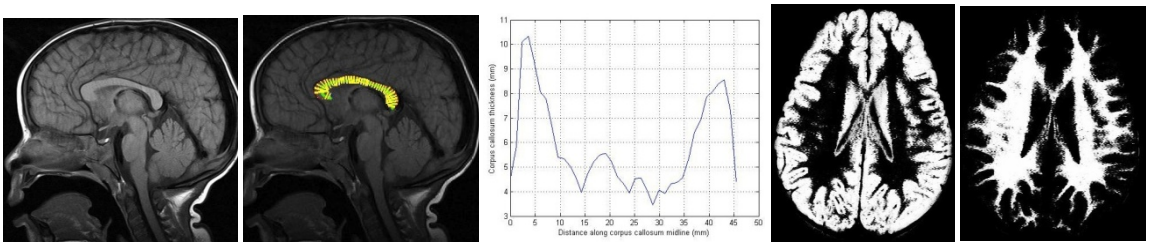


Figure 3.2. Patient 2- Sagittal T1, corpus callosum radial thickness measurements, thickness graph, GM and WM segmentation

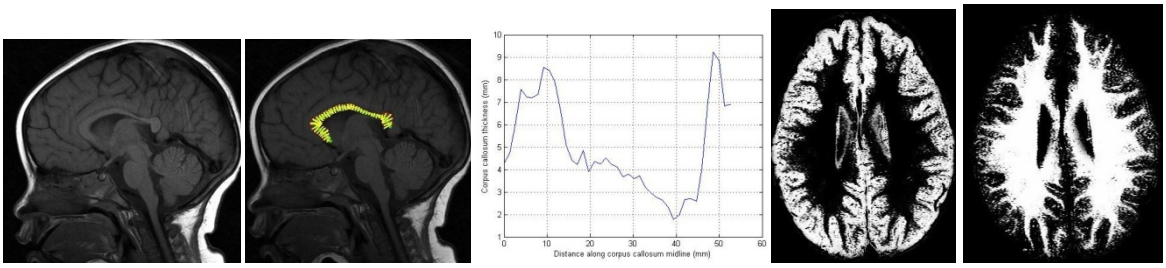


Figure 3.3. Patient 3- Sagittal T1, corpus callosum radial thickness measurements, thickness graph, GM and WM segmentation

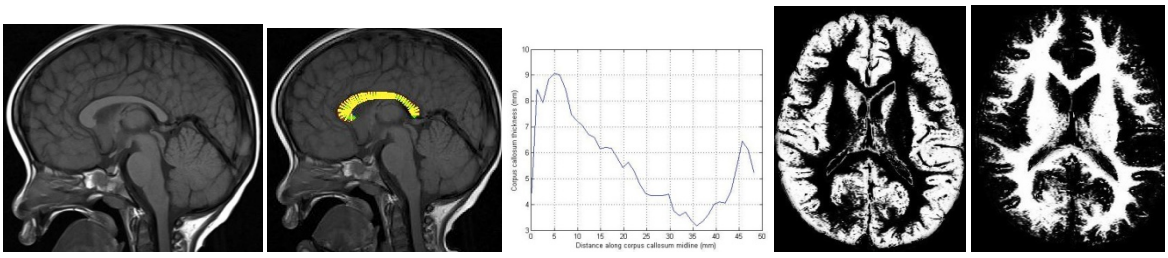


Figure 3.4. Patient 4- Sagittal T1, corpus callosum radial thickness measurements, thickness graph, GM and WM segmentation

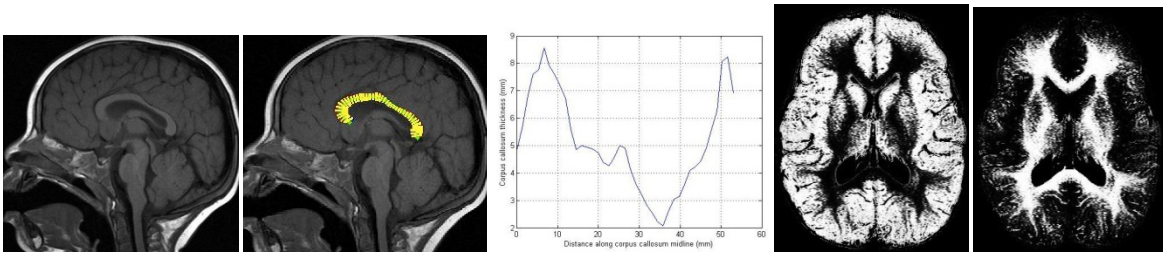


Figure 3.5. Patient 5- Sagittal T1, corpus callosum radial thickness measurements, thickness graph, GM and WM segmentation

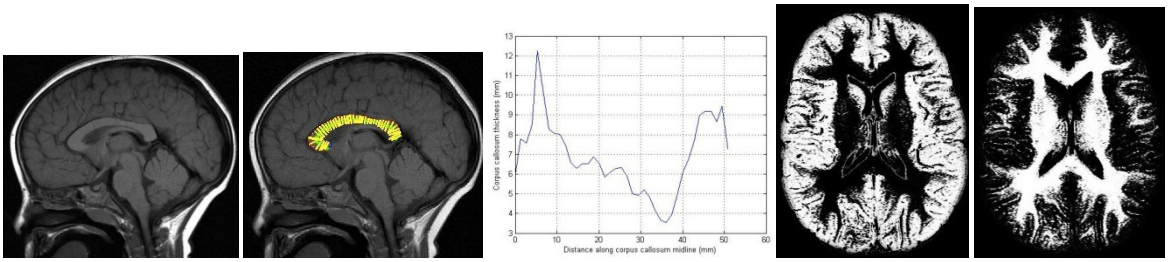


Figure 3.6. Patient 6- Sagittal T1, corpus callosum radial thickness measurements, thickness graph, GM and WM segmentation

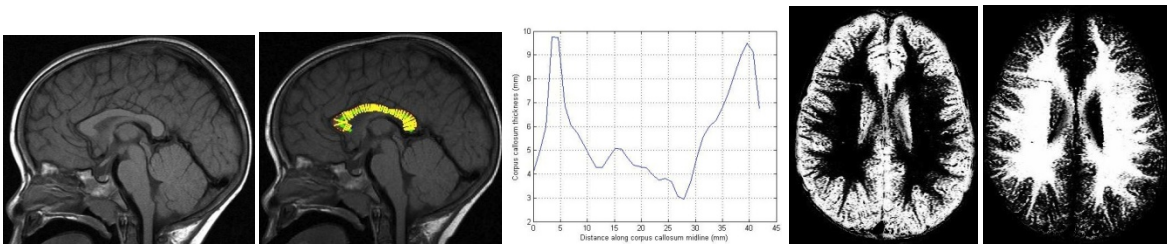


Figure 3.7. Patient 7- Sagittal T1, corpus callosum radial thickness measurements, thickness graph, GM and WM segmentation

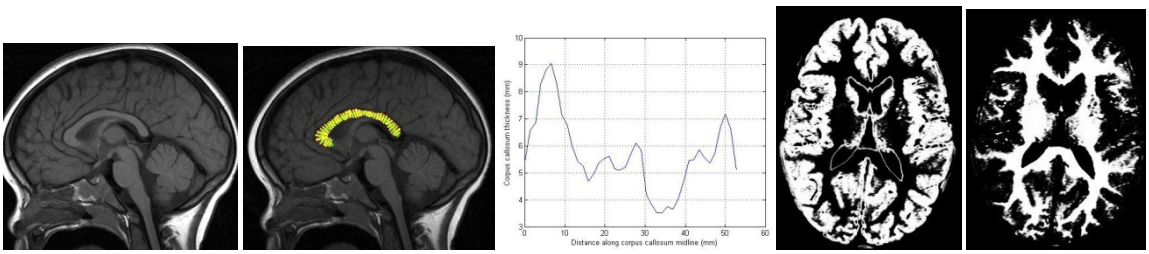


Figure 3.8. Patient 8- Sagittal T1, corpus callosum radial thickness measurements, thickness graph, GM and WM segmentation

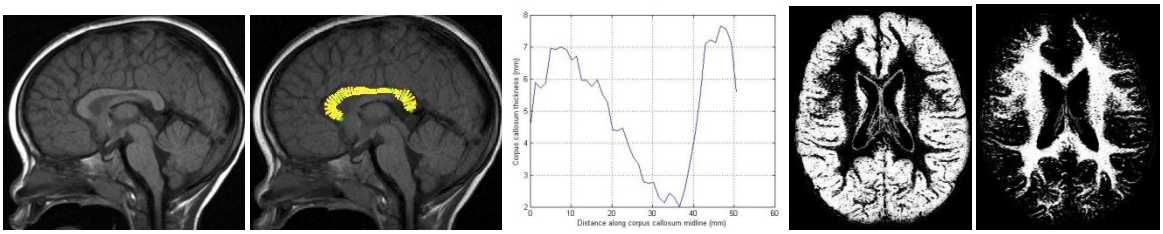


Figure 3.9. Patient 9- Sagittal T1, corpus callosum radial thickness measurements, thickness graph, GM and WM segmentation

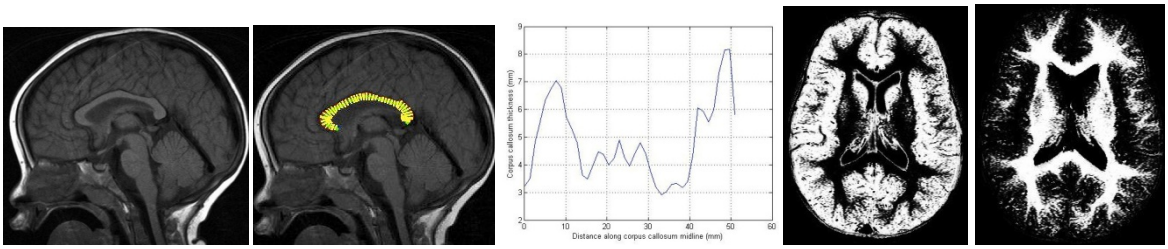


Figure 3.10. Patient 10- Sagittal T1, corpus callosum radial thickness measurements, thickness graph, GM and WM segmentation

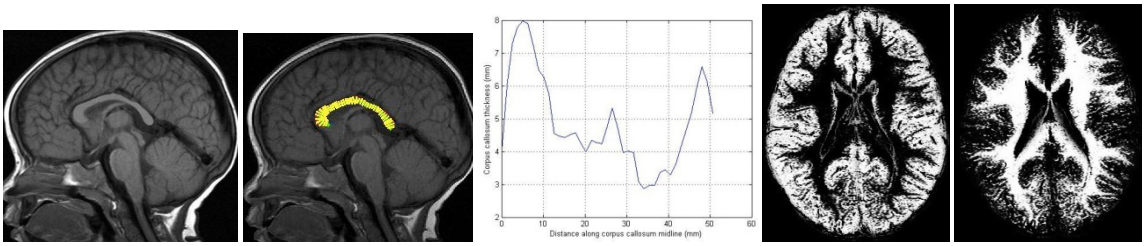


Figure 3.11. Patient 11- Sagittal T1, corpus callosum radial thickness measurements, thickness graph, GM and WM segmentation

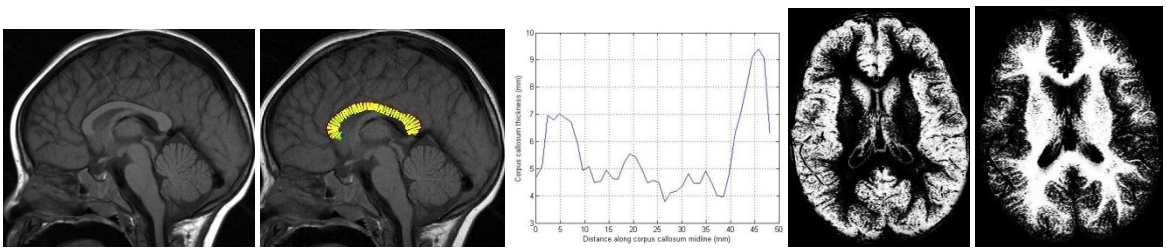


Figure 3.12. Patient 12- Sagittal T1, corpus callosum radial thickness measurements, thickness graph, GM and WM segmentation

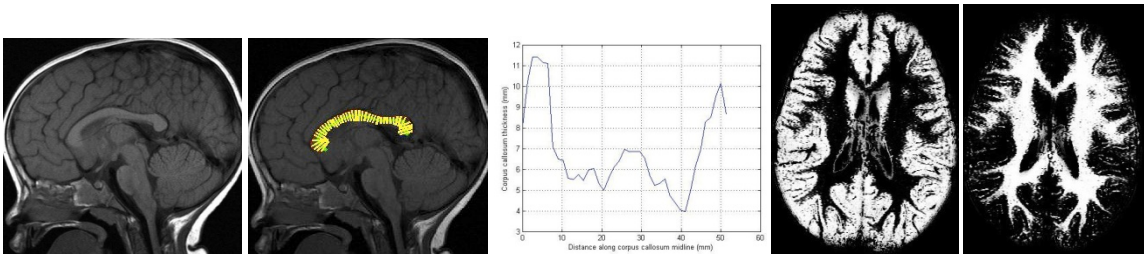


Figure 3.13. Patient 13- Sagittal T1, corpus callosum radial thickness measurements, thickness graph, GM and WM segmentation

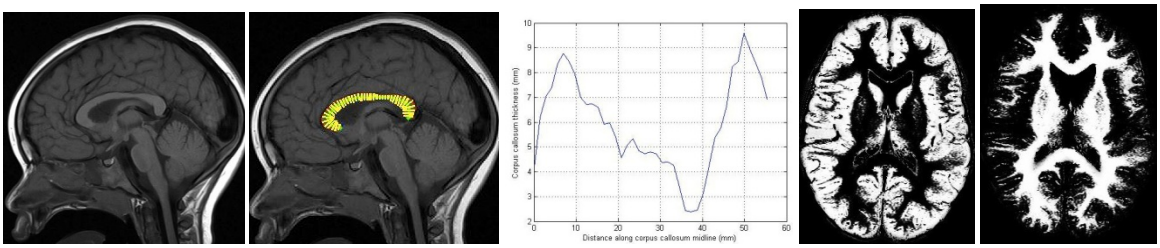


Figure 3.14. Patient 14- Sagittal T1, corpus callosum radial thickness measurements, thickness graph, GM and WM segmentation

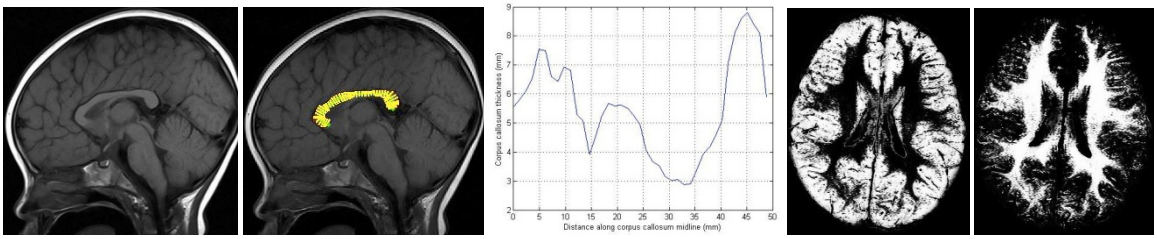


Figure 3.15. Patient 15- Sagittal T1, corpus callosum radial thickness measurements, thickness graph, GM and WM segmentation

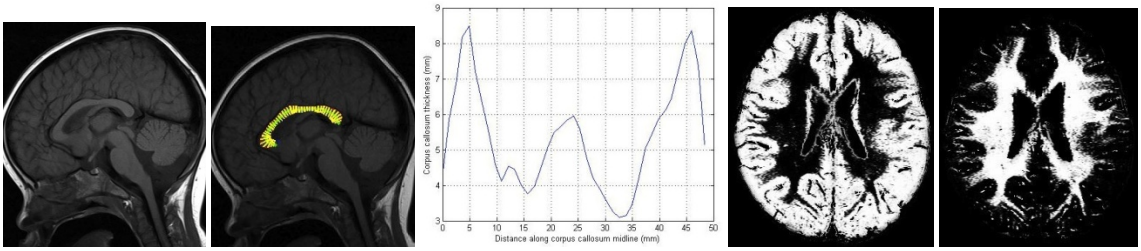


Figure 3.16. Patient 16- Sagittal T1, corpus callosum radial thickness measurements, thickness graph, GM and WM segmentation

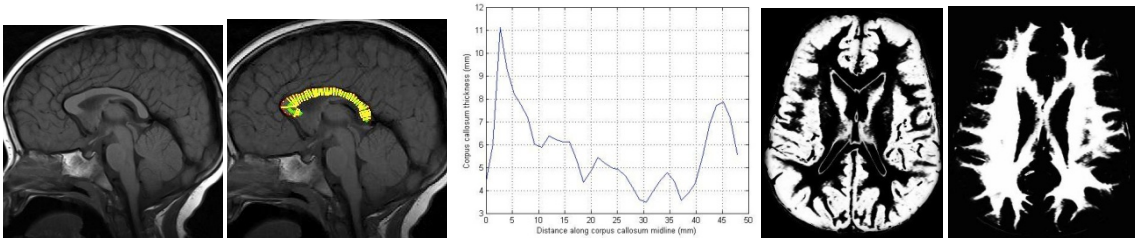


Figure 3.17. Patient 17- Sagittal T1, corpus callosum radial thickness measurements, thickness graph, GM and WM segmentation

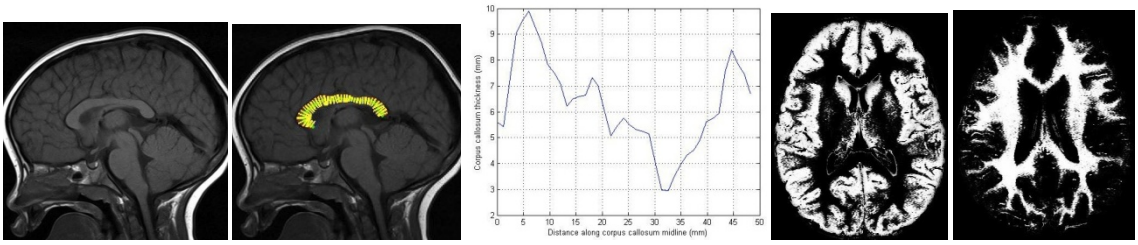


Figure 3.18. Patient 18- Sagittal T1, corpus callosum radial thickness measurements, thickness graph, GM and WM segmentation

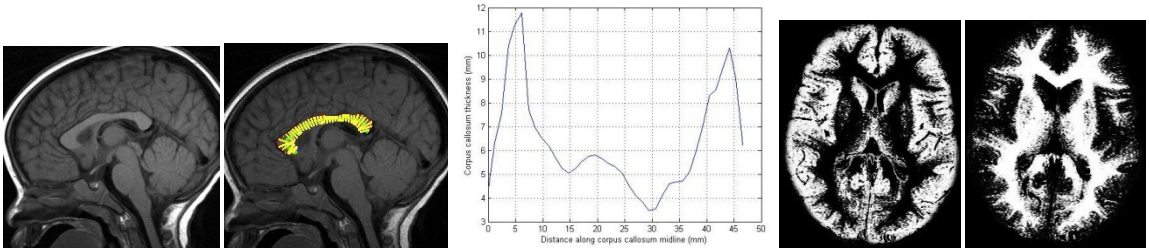


Figure 3.19. Patient 19- Sagittal T1, corpus callosum radial thickness measurements, thickness graph, GM and WM segmentation

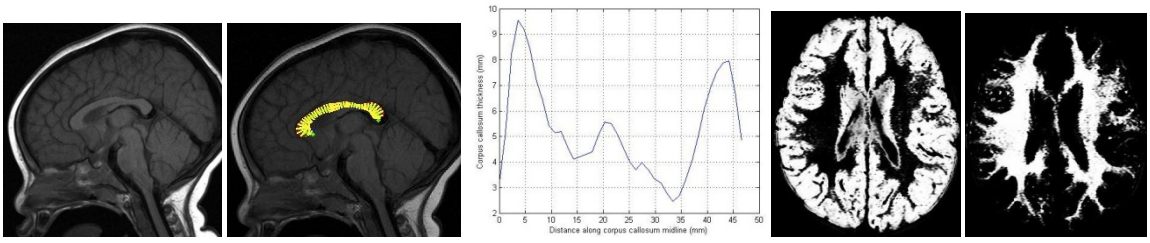


Figure 3.20. Patient 20- Sagittal T1, corpus callosum radial thickness measurements, thickness graph, GM and WM segmentation

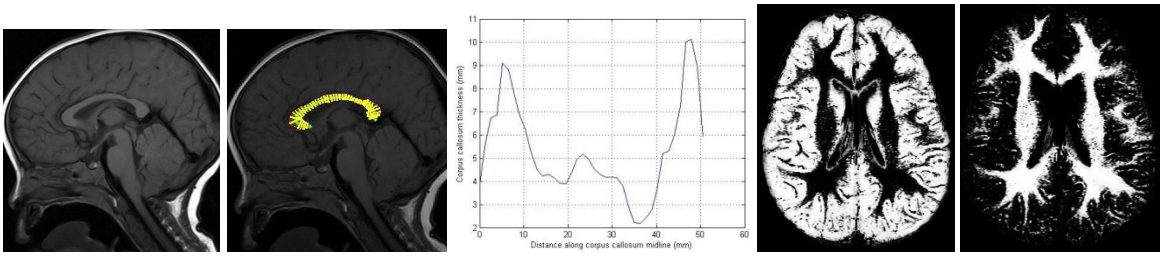


Figure 3.21. Patient 21- Sagittal T1, corpus callosum radial thickness measurements, thickness graph, GM and WM segmentation

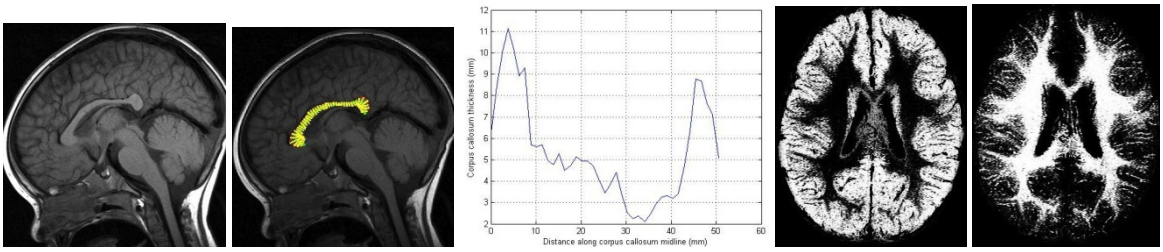


Figure 3.22. Patient 22- Sagittal T1, corpus callosum radial thickness measurements, thickness graph, GM and WM segmentation

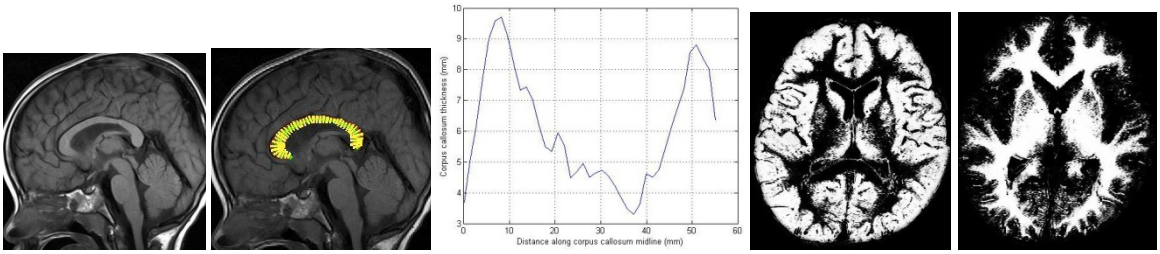


Figure 3.23. Patient 23- Sagittal T1, corpus callosum radial thickness measurements, thickness graph, GM and WM segmentation

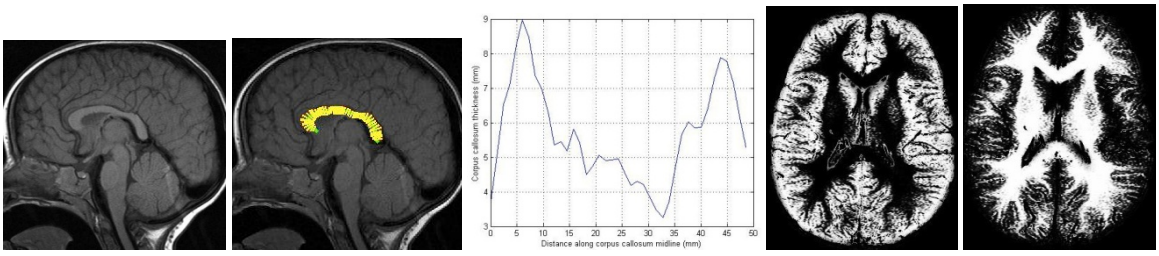


Figure 3.24. Patient 24- Sagittal T1, corpus callosum radial thickness measurements, thickness graph, GM and WM segmentation

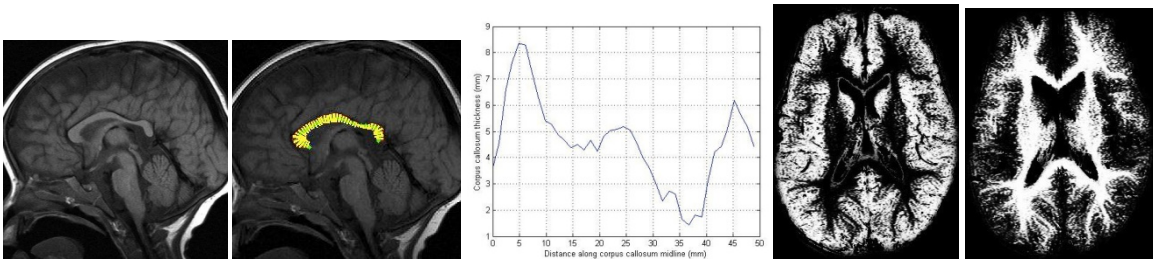


Figure 3.25. Patient 25- Sagittal T1, corpus callosum radial thickness measurements, thickness graph, GM and WM segmentation

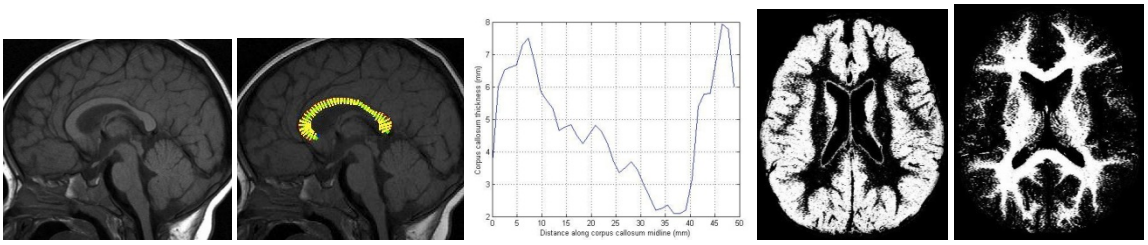


Figure 3.26. Patient 26- Sagittal T1, corpus callosum radial thickness measurements, thickness graph, GM and WM segmentation

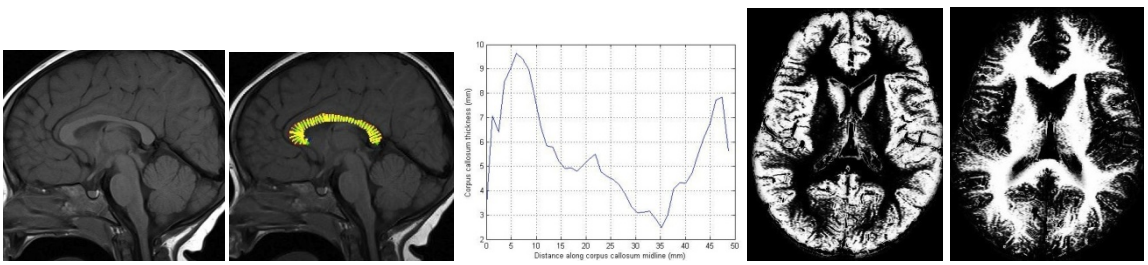


Figure 3.27. Patient 27- Sagittal T1, corpus callosum radial thickness measurements, thickness graph, GM and WM segmentation

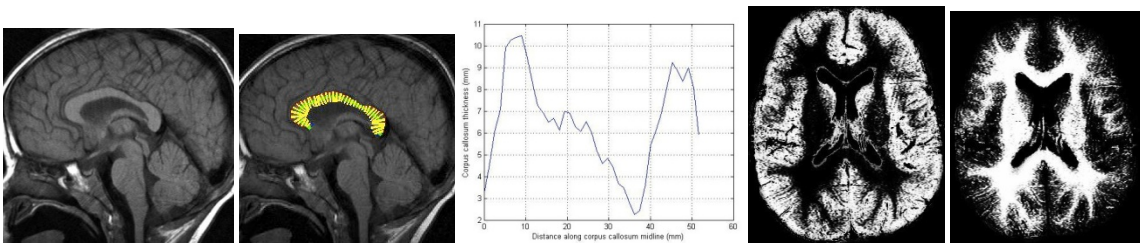


Figure 3.28. Patient 28- Sagittal T1, corpus callosum radial thickness measurements, thickness graph, GM and WM segmentation

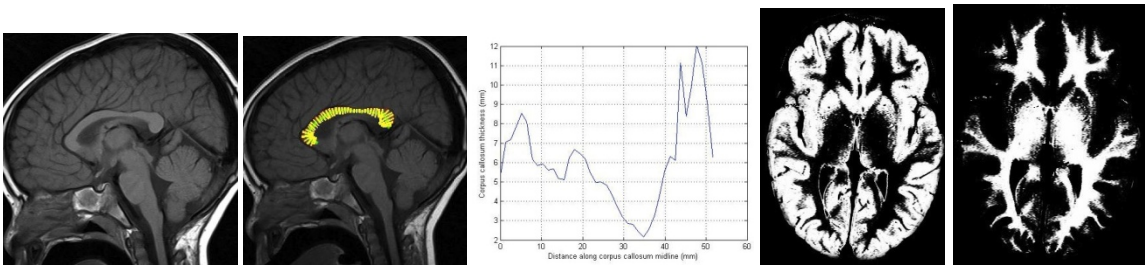


Figure 3.29. Patient 29- Sagittal T1, corpus callosum radial thickness measurements, thickness graph, GM and WM segmentation

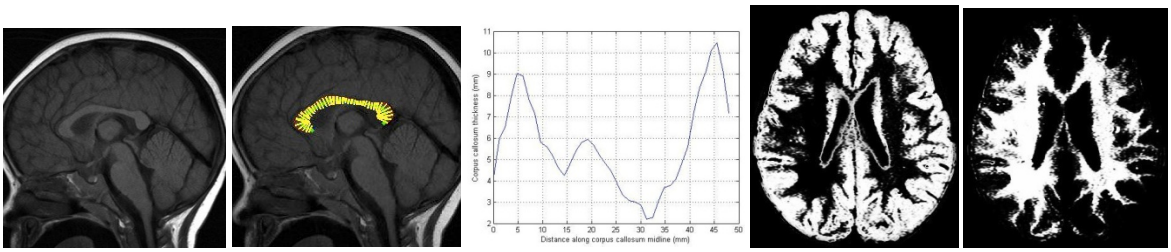


Figure 3.30. Patient 30- Sagittal T1, corpus callosum radial thickness measurements, thickness graph, GM and WM segmentation

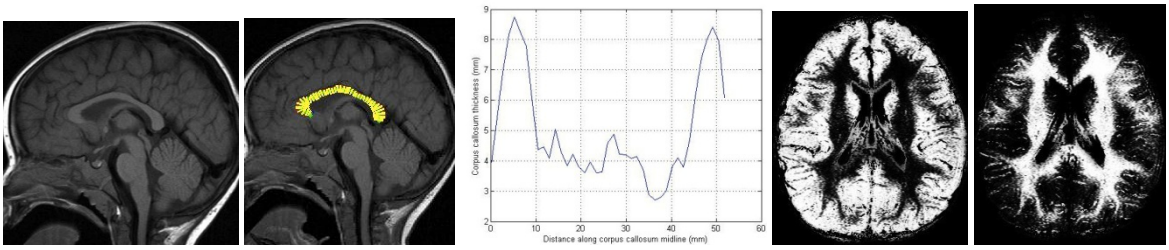


Figure 3.31. Patient 31- Sagittal T1, corpus callosum radial thickness measurements, thickness graph, GM and WM segmentation

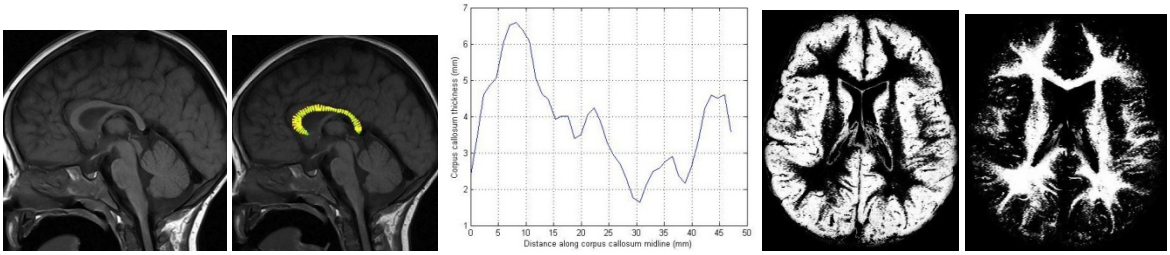


Figure 3.32. Patient 32- Sagittal T1, corpus callosum radial thickness measurements, thickness graph, GM and WM segmentation

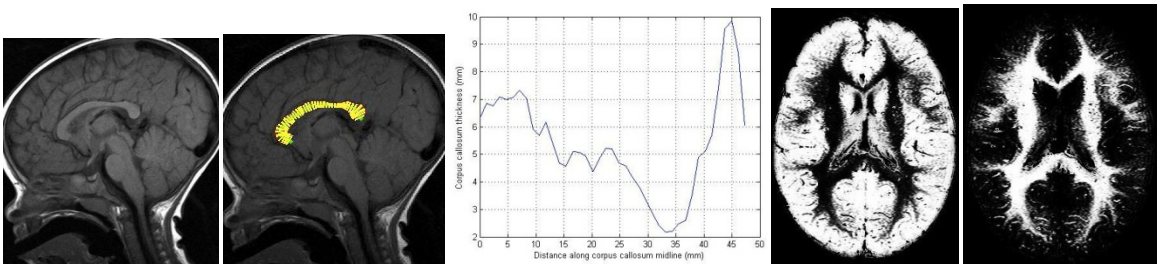


Figure 3.33. Patient 33- Sagittal T1, corpus callosum radial thickness measurements, thickness graph, GM and WM segmentation

3.2. Results of clinical findings

3.2.1. Griffiths Mental Development Scores (GMDS)

Griffiths Mental Development Score (GMDS) determination was not possible in two of the patients. Means were therefore calculated for 31 patients. Mental development score assessments were performed at a mean age of 30 months (range 11-48 months), within a mean of three months (range four days – six months) of the neuroimaging date. GMDS scores for patients are summarised in Table 3.4.

Table 3.4. Summary Statistics for Griffiths Mental Development Score (GMDS) : General Quotient (GQ) and Sub Scores (Locomotor and Language)(Patients Only)

GMDS	N	Min	Max	Median	25th Centile	75 Centile	Mean	Std Dev.
GQ	31	72	101	84	79	88	84	7
Locomotor	31	59	116	83	76.2	89	84	13
Language	31	57	118	79	73.6	86	80	12

Key: GMDS = Griffiths General Mental Development Score; GQ = general quotient

Mean normal values for the Griffiths Mental Development Scale in South African children are: GQ 100.2; Locomotor 100.4 and Language 99.8 (49). Mean scores in patients fell into the 'low average' category with the mean GQ of 84 (range 72 – 101). The 'locomotor' sub-score mean was 84 (range 59 – 116) and the 'language' sub-score mean was 80 (range 57 – 118).

3.2.2. Clinical and Laboratory Parameters

Clinical parameters including time on HAART, nadir CD4 and CD4 closest to the time of the MRI are summarised in Table 3.5.

Table 3.5. Summary Statistics of clinical and laboratory parameters (Patients only)

Variable	N	Min	Max	Median	25th Percentile	75th Percentile	Mean	SD.
Time on HAART (days)	33	24	199	102	80.4	144	108	46
Nadir CD4 %	33	12	35	21.4	16.6	26	21	6
Nadir CD4 count	33	268	3055	1099	823	1639	1201	627
CD4 % closest to scan	33	19	53	34	29.9	40.2	34	9
CD4 count closest to scan	33	644	3558	1403	1026	1766	1522	718

Correlations and comparisons

Table 3.6 tabulates the correlations between the various measurements of the corpus callosum with age. The only significant correlation with age was for premotor CC (mean) where there was a positive association, significant at 5 % level.

Table 3.6. Correlation of corpus callosum measurements with age

Variable	Age	
	Correlation Coefficient	Significance
Whole CC (mean)	0.1655	0.283
Whole CC (max)	-0.0521	0.737
Prefrontal CC (mean)	0.0262	0.8661
Prefrontal CC (max)	0.0031	0.984
Premotor CC (mean)	**0.3089**	**0.0413**
Premotor CC (max)	0.1624	0.2921
Motor CC (mean)*	0.1939	0.2072
Motor CC (max)*	0.2286	0.1355
Sensory CC (mean)*	0.1123	0.4682
Sensory CC (max)	0.0772	0.6184
Visual CC (mean)	0.0293	0.85
Visual CC (max)	-0.0362	0.8156
CC length	0.1963	0.2017
Total brain volume	0.029	0.852
White matter volume	-0.0714	0.6453
Grey matter volume	0.0782	0.6138

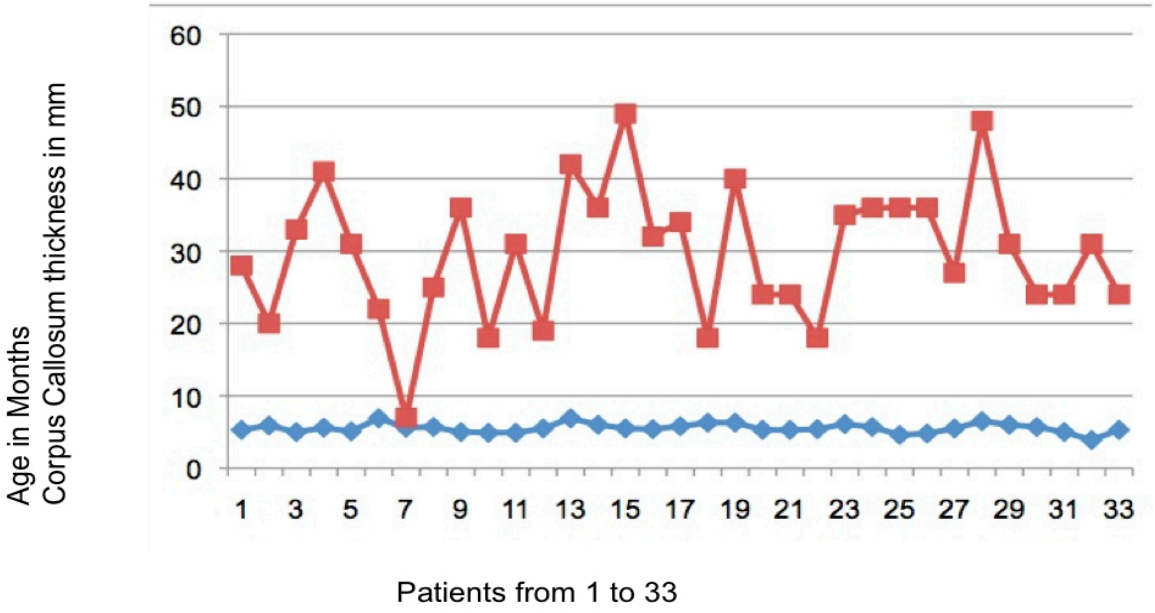
Note: * = Spearman

3.3. Results of comparison of patients with controls

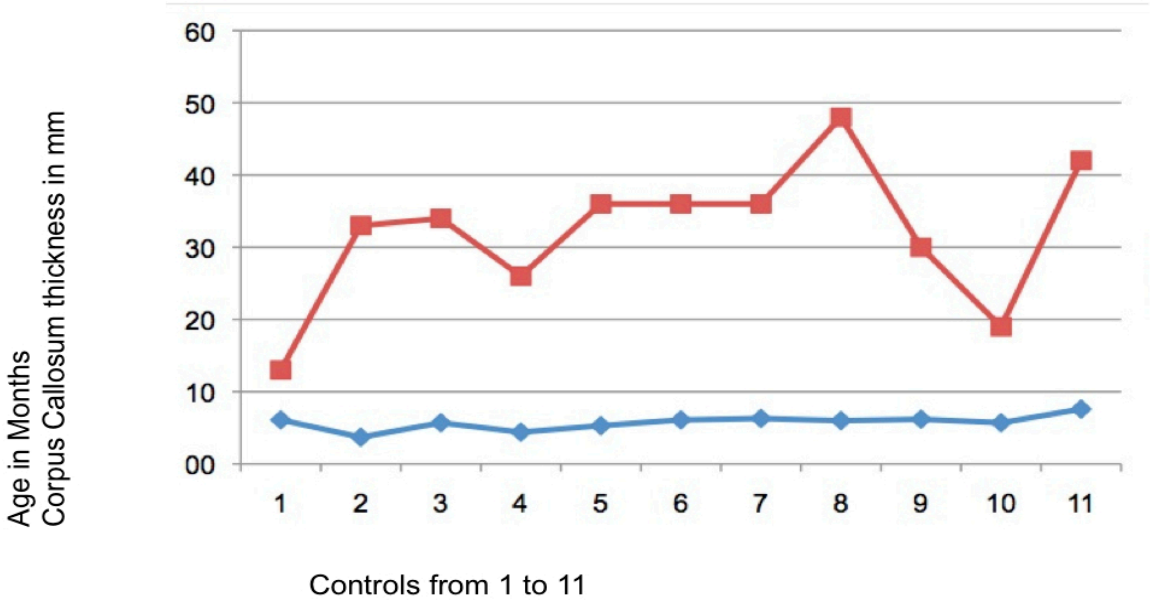
'Overall mean CC thickness' for patients and controls is graphically presented in Figures 3.34 (a) and (b) below.

Figures 3.34 a and b: Graphic representation of (a) Individual patients and (b) controls mean corpus callosum thickness in mm (blue diamonds) vs. age in months (red blocks)

(a)

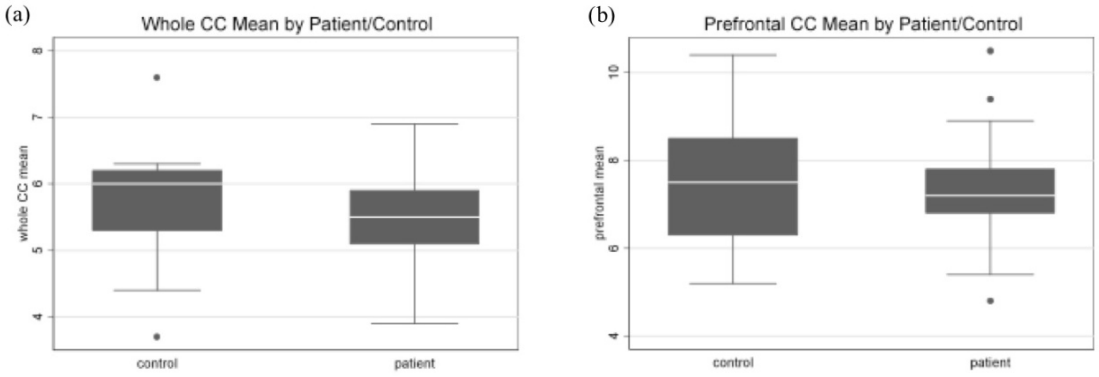


(b)

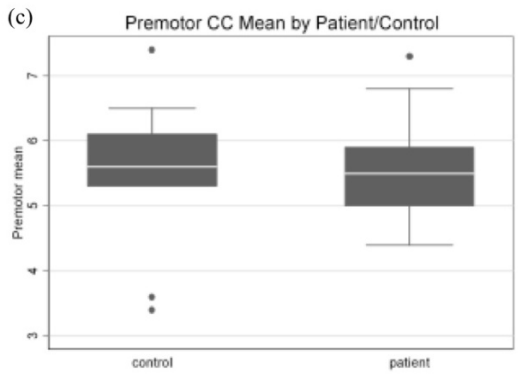


Box and whisker plots Figure 3.35 (a) – (f) below compare mean values of CC thickness between patients and controls. There were no statistical differences between the values obtained for the patients and those obtained for the controls:

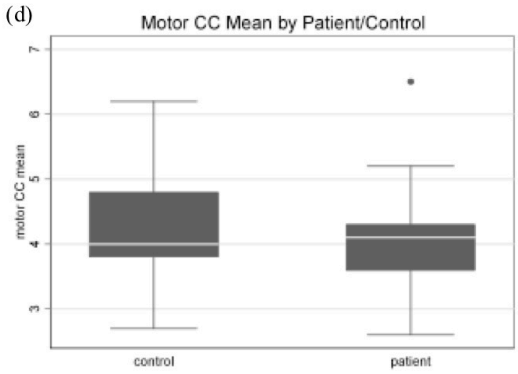
Figure 3.35 a – f: Box and whisker plots comparing mean values of corpus callosum thickness between patients and controls



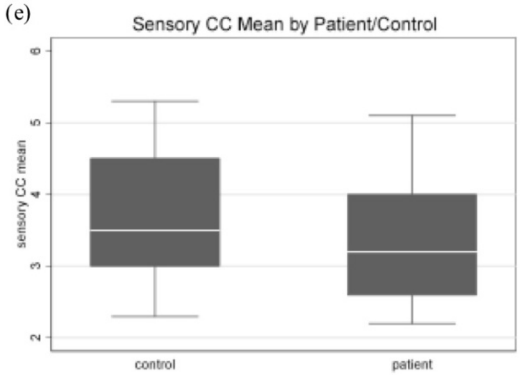
p=0.45 **p=0.82**



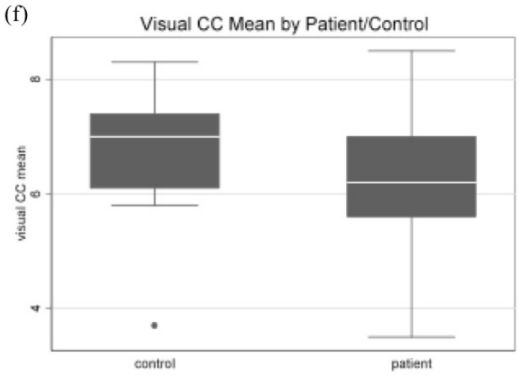
p = 0.92



p=0.81



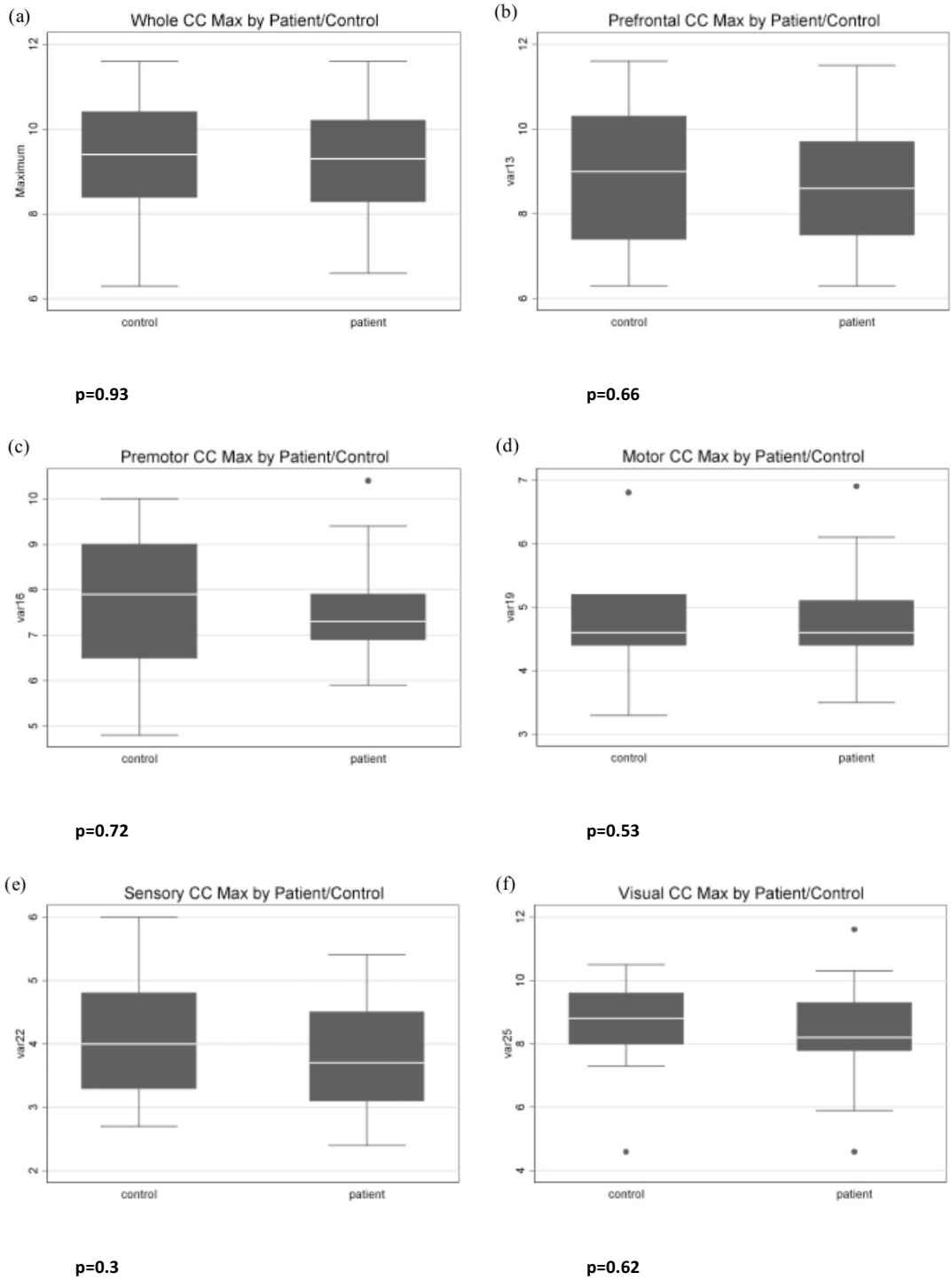
p=0.60



p=0.23

Box and whisker plots Figure 3.36 (a) – (f) below compare maximum values of regional CC thickness between patients and controls.

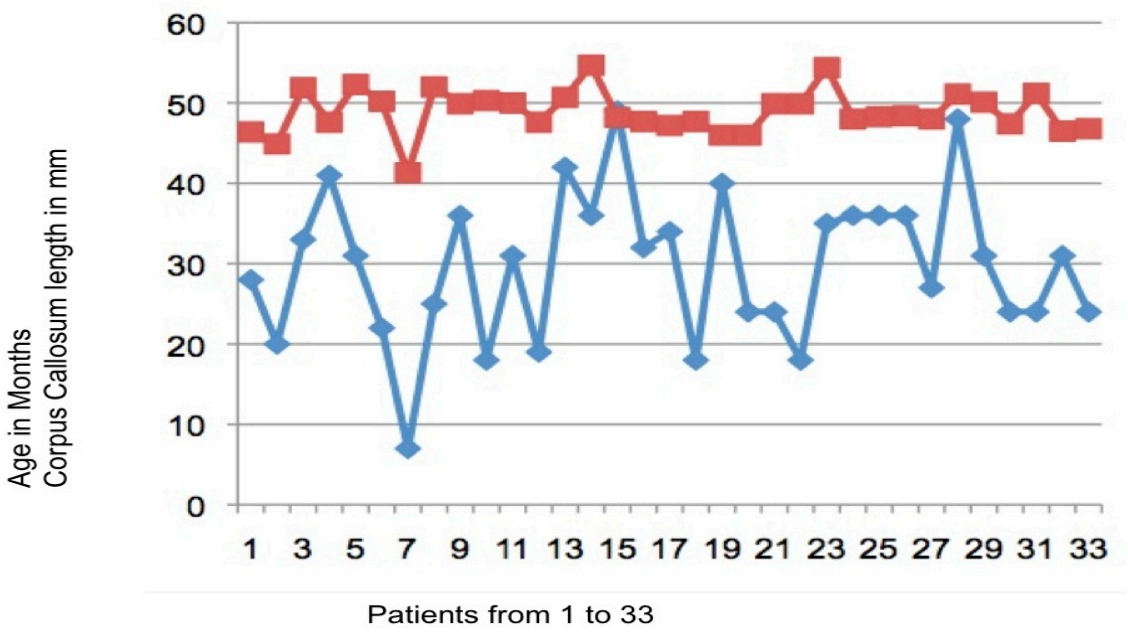
Figure 3.36 a - f: Box and whisker plots comparing maximum values of regional corpus callosum thickness (a) whole corpus callosum, (b) prefrontal corpus callosum, (c) premotor corpus callosum, (d) motor corpus callosum, (e) sensory corpus callosum and (f) visual corpus callosum between patients and controls



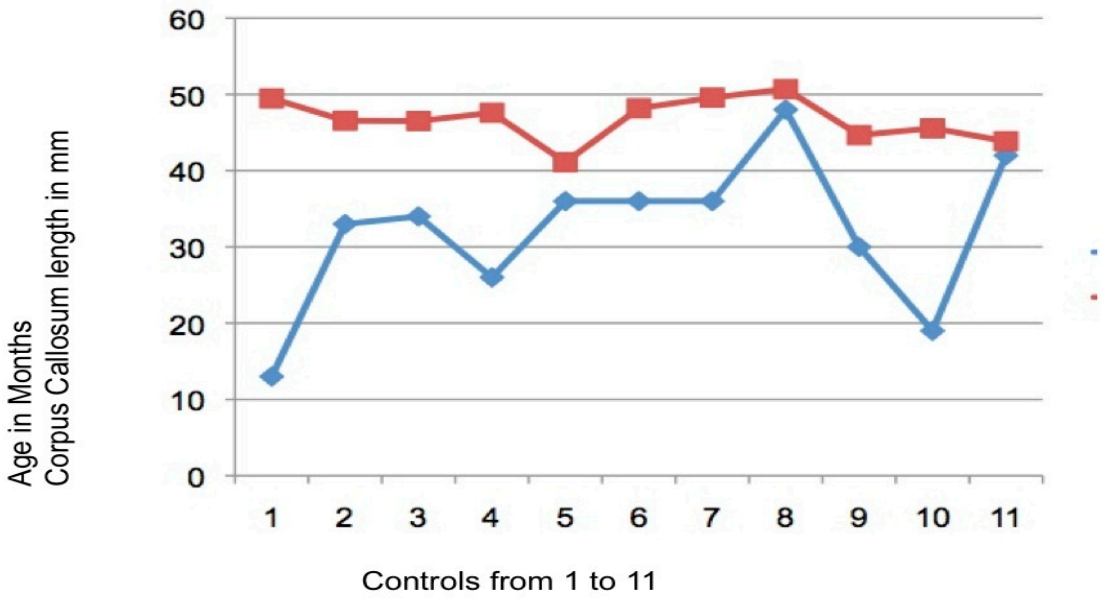
CC length was generally greater in patients than controls [Patients mean 48.9 mm (SD 2.7); Controls mean 46.7 mm (SD 2.8)]. CC length vs. age in months is graphically represented for patients and controls in Figure 3.37 (a) and (b) respectively below:

Figure 3.37. (a) Patients and (b) controls mean corpus callosum length in mm (red blocks) vs. age in months (blue diamonds)

(a)

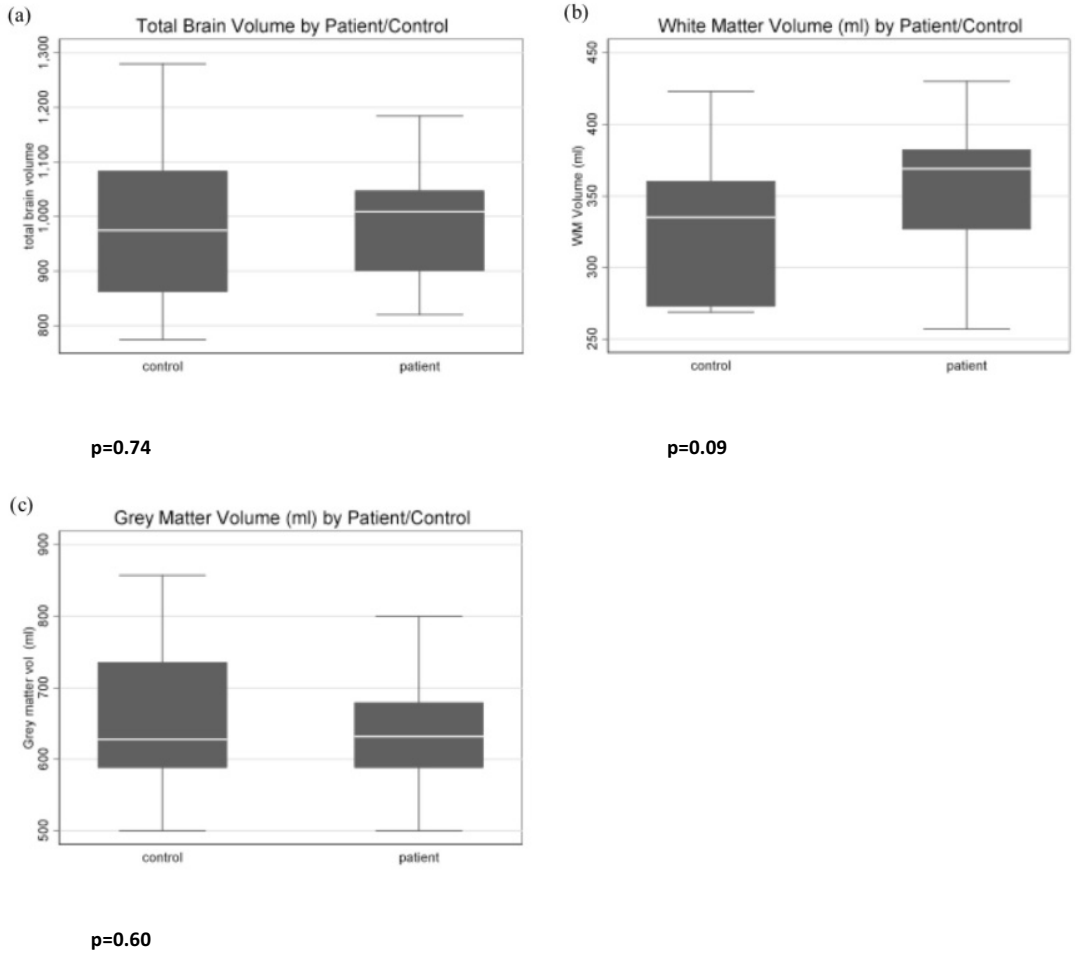


(b)



Box and whisker plots Figure 3.38 (a) – (c) below compare brain volumes between patients and controls:

Figure 3.38. Box and whisker plots comparing brain volumes (a) TBV, (b) WMV and (c) GMV between patients and controls



Comparison of controls with patients utilizing the t-test for normally distributed variables and the Wilcoxon rank sum test for non-normally distributed variables is summarised with regard to CC thickness means, maximums and brain volumes in Tables 3.7 (a) and (b) below.

Table 3.7 (a) means and (b) maximums: t-test results for normally distributed variables [Overall corpus callosum, Prefrontal corpus callosum, Premotor corpus callosum, Visual corpus callosum, Sensory corpus callosum (max only), total brain volume, white matter volume and grey matter volume]

(a) Means

Variable	Group	N	Group Mean	t-Test Value	Significance (Two-sided)
Whole CC (mean)	Controls	11	5.7	0.7673	0.4472
	Patients	33	5.5		
Prefrontal CC (mean)	Controls	11	7.4	0.2347	0.8156
	Patients	33	7.3		
Premotor CC (mean)	Controls	11	5.5	-0.0969	0.9233
	Patients	33	5.5		
Visual CC (mean)	Controls	11	6.7	1.2239	0.2278
	Patients	33	6.2		
Total Brain Volume	Controls	11	974.2	-0.3303	0.7428
	Patients	33	986.8		
White matter volume	Controls	11	326.9	-1.7166	0.0934
	Patients	33	354.9		
Grey matter volume	Controls	11	647.4	0.5262	0.6015
	Patients	33	631.9		

(b) Maximums

Variable	Group	N	Group Mean	t-Test Value	Significance (Two-sided)
Whole CC (max)	Controls	11	9.4	0.0853	0.9324
	Patients	33	9.3		
Prefrontal CC (max)	Controls	11	9	0.442	0.6608
	Patients	33	8.7		
Premotor CC (max)	Controls	11	7.6	0.3622	0.719
	Patients	33	7.5		
Visual CC (max)	Controls	11	8.6	0.4976	0.6213
	Patients	33	8.4		
Sensory CC (max)	Controls	11	4.1	1.0521	0.2988
	Patients	33	3.7		

None of the differences in CC thickness and brain volume between patients and controls were statistically significant. The results of the Wilcoxon rank sum test used for non-normal variables are summarized in Table 3.8 below and show no significant differences.

Table 3.8. Wilcoxon test for non-normally distributed variables (Motor corpus callosum, Sensory corpus callosum)

Variable	Group	N	Group Median	Z-Test Value	Significance (Two-sided)	Probability that Control>Patient
Motor CC (mean)	Controls	11	4	0.245	0.8067	0.525
	Patients	33	4.1			
Motor CC (max)	Controls	11	4.6	0.299	0.765	0.53
	Patients	33	4.6			
Sensory CC (mean)	Controls	11	3.5	0.991	0.3219	0.601
	Patients	33	3.2			

3.4. Results of correlations of MRI features (corpus callosum thickness, length, brain volumes) with each other and with clinical / laboratory parameters

Correlations of CC thickness and length with brain volume (TBV, WMV and GMV) are shown in Table 3.9 below, with values in bold and red indicating significance at the 5 % level.

Table 3.9. Correlation of corpus callosum thickness (mean and maximum) and corpus callosum length with brain volume measurements (TBV, WMV, GMV)

Variable	Total Brain Volume		White matter volume		Grey matter volume	
	Correlation Coefficient	Significance	Correlation Coefficient	Significance	Correlation Coefficient	Significance
Whole CC (mean)	**0.2992**	**0.0485**	0.2834	0.0623	0.2237	0.1444
Whole CC (max)	0.1532	0.3206	0.1879	0.2219	0.0901	0.5608
Prefrontal CC (mean)	0.2125	0.1661	0.263	0.0845	0.1235	0.4243
Prefrontal CC (max)	0.2612	0.0867	**0.3528**	**0.0188**	0.135	0.3823
Premotor CC (mean)	**0.3126**	**0.0388**	**0.3536**	**0.0185**	0.2008	0.1913
Premotor CC (max)	0.2693	0.0771	**0.3429**	**0.0227**	0.1511	0.3277
Motor CC (mean)*	0.2032	0.1859	0.1787	0.2458	0.115	0.4575
Motor CC (max)*	0.241	0.1151	0.234	0.1263	0.1098	0.478
Sensory CC (mean)*	**0.3457**	**0.0215**	0.2573	0.0917	0.234	0.1264
Sensory CC (max)	0.2676	0.0791	0.2677	0.0789	0.1919	0.212
Visual CC (mean)	0.2117	0.1678	0.1109	0.4736	0.2095	0.1723
Visual CC (max)	0.0284	0.8549	-0.0121	0.9379	0.0435	0.779
CC length	0.0724	0.6407	0.1046	0.499	0.0334	0.8295

Note: * = Spearman

Total brain volume and white matter volume correlated positively and significantly with a few of the corpus callosum measurements, but there were no consistent correlations across all three brain volume measurements.

Correlations of CC thickness (and length) in patients only, with clinical and laboratory parameters are shown in Tables 3.10, 3.11 and 3.12 below, with values in bold and red indicating significance at the 5 % level.

Table 3.10. Correlation of corpus callosum thickness (mean and maximum) with Griffiths Mental Development Scores

Variable	General Quotient (GQ)		Locomotor		Language*	
	Correlation Coefficient	Significance	Correlation Coefficient	Significance	Correlation Coefficient	Significance
Whole CC (mean)	-0.1325	0.4773	-0.1615	0.3856	0.0513	0.7839
Whole CC (max)	-0.0421	0.8221	-0.0035	0.9851	0.0898	0.6311
Prefrontal CC (mean)	-0.1791	0.3351	-0.0551	0.7685	0.0517	0.7826
Prefrontal CC (max)	-0.1038	0.5783	-0.2036	0.2719	0.0695	0.7101
Premotor CC (mean)	-0.1606	0.3881	-0.0844	0.6516	-0.1315	0.4806
Premotor CC (max)	-0.111	0.5521	-0.0334	0.8585	-0.1515	0.4159
Motor CC (mean)*	-0.3408	0.0606	-0.2042	0.2706	-0.0576	0.7582
Motor CC (max)*	**-0.3954**	**0.0277**	-0.0997	0.5938	-0.144	0.4395
Sensory CC (mean)*	-0.1682	0.3658	-0.1972	0.2877	-0.012	0.9488
Sensory CC (max)	-0.1589	0.3932	-0.2513	0.1727	0.0142	0.9398
Visual CC (mean)	0.156	0.402	-0.057	0.7606	0.2789	0.1287
Visual CC (max)	0.1518	0.415	0.1005	0.5907	0.1918	0.3012

Note: * = Spearman

Table 3.11. Correlation of CC thickness (mean and maximum) with clinical / laboratory parameters

Variable	Failure of brain growth		Time on HAART		Nadir CD4	
	Correlation Coefficient	Significance	Correlation Coefficient	Significance	Correlation Coefficient	Significance
Whole CC (mean)	-0.1265	0.4832	-0.1517	0.3994	0.0559	0.7572
Whole CC (max)	-0.017	0.9253	-0.2436	0.1719	0.3216	0.068
Prefrontal CC (mean)	0.0688	0.7034	-0.245	0.1694	0.268	0.1316
Prefrontal CC (max)	-0.0457	0.8006	-0.3322	0.0589	0.3498	0.046
Premotor CC (mean)	-0.0939	0.6034	-0.0071	0.9688	-0.0443	0.8065
Premotor CC (max)	0.0898	0.6193	0.0249	0.8905	0.0638	0.7245
Motor CC (mean)*	0.1028	0.569	0.06	0.7401	-0.1292	0.4736
Motor CC (max)*	0.1193	0.5083	0.0522	0.7728	-0.1996	0.2654
Sensory CC (mean)*	-0.1954	0.2758	-0.121	0.5025	0.1456	0.4189
Sensory CC (max)	-0.2446	0.1701	-0.1304	0.4696	0.1604	0.3725
Visual CC (mean)	-0.2679	0.1317	-0.1571	0.3826	-0.041	0.8209
Visual CC (max)	-0.1039	0.565	-0.1439	0.4243	0.0576	0.7502

Note: * = Spearman

Table 3.12. Correlation of corpus callosum thickness (mean and maximum) with laboratory parameters (nadir CD4, CD4 closest to scan)

Variable	Nadir CD4 Count*		CD4 closest to scan		CD4 closest to scan*	
	Correlation Coefficient	Significance	Correlation Coefficient	Significance	Correlation Coefficient	Significance
Whole CC (mean)	0.0113	0.9502	-0.1777	0.3225	0.0253	0.8889
Whole CC (max)	0.176	0.3271	0.0491	0.7861	0.2163	0.2268
Prefrontal CC (mean)	0.0933	0.6054	0.13	0.471	0.3336	0.0578
Prefrontal CC (max)	0.2033	0.2566	0.1379	0.444	0.2461	0.1675
Premotor CC (mean)	-0.0095	0.9583	-0.2486	0.163	-0.0352	0.846
Premotor CC (max)	0.3049	0.0845	-0.1018	0.5729	-0.1395	0.4388
Motor CC (mean)*	-0.0562	0.7559	-0.2127	0.2347	0.0106	0.9535
Motor CC (max)*	-0.2681	0.1314	-0.1378	0.4443	-0.0899	0.6187
Sensory CC (mean)*	0.0544	0.7637	-0.1521	0.3981	0.0654	0.7176
Sensory CC (max)	-0.0064	0.9716	-0.0343	0.8497	0.0649	0.7196
Visual CC (mean)	-0.0622	0.7308	-0.1553	0.3881	-0.195	0.2767
Visual CC (max)	0.1256	0.4862	-0.0579	0.7489	-0.0367	0.8395

Note: * = Spearman

Correlations of CC length (only in patients) with clinical and laboratory parameters are shown in Table 3.13 below, with values in bold and red indicating significance at the 5 % level.

Table 3.13. Correlation of corpus callosum length and clinical / laboratory parameters (patients only)

Variable	CC length	
	Correlation Coefficient	Significance
General	-0.2112	0.2542
Locomotor	0.1662	0.3714
Language*	-0.1035	0.5796
Time on HAART	0.1833	0.3072
Nadir CD4	-0.2083	0.2446
Nadir CD4 Count*	-0.1725	0.3533
CD4 closest to scan	-0.2458	0.168
CD4 count closest to scan *	**-0.3709**	**0.04**

Note: * = Spearman

Correlations of brain volumes (only in patients) with clinical and laboratory parameters are shown in Table 3.14 below.

Table 3.14. Correlation of brain volumes with clinical parameters (GMDS and microcephaly) and laboratory parameters (time on HAART and CD4)

Variable	Total Brain Volume		White matter volume		Grey matter volume	
	Correlation Coefficient	Significance	Correlation Coefficient	Significance	Correlation Coefficient	Significance
General	-0.0875	0.6399	-0.2148	0.2458	0.0281	0.8806
Locomotor	-0.158	0.396	-0.1968	0.2885	-0.0706	0.706
Language*	-0.1111	0.552	-0.0071	0.9699	-0.0878	0.6387
Microcephaly	0.0072	0.9684	0.0839	0.6425	-0.0412	0.82
Time on HAART	-0.159	0.3767	-0.1225	0.497	-0.123	0.4952
NADIR CD4	0.3301	0.0606	0.1544	0.3909	0.3148	0.0743
NADIR CD4 Count*	0.0196	0.9168	-0.115	0.538	0.0994	0.5946
CD4 closest to scan	-0.161	0.3706	0.0949	0.5995	-0.2551	0.152
CD4 count closest to scan *	-0.0871	0.6413	0.1022	0.5842	-0.1944	0.2946

Note: * = Spearman

Inter-class correlation and standard error of measurement of two different operators generating measurements using the software is summarized in table 3.15 below.

Table 3.15. Inter-class correlation and standard error of measurement of two different operators generating measurements using the software

	ICC	SEM
Length	0.31	2.47
Overall thickness	0.80	0.348
Prefrontal section measurement	0.86	0.44
Premotor section measurement	0.77	0.33
Motor section measurement	0.74	0.39
Sensory section measurement	0.59	0.58
Visual section measurement	0.67	0.83

These findings indicate poor correlation between observers for length, visual and sensory measurements while the other inter-observer measurement correlations were reasonable.

4. Discussion

This study correlated thickness and length of the CC with brain volume. To achieve this, specific semi-automated software was created to yield multiple measures of thickness and a single measure of length of the CC for each patient and control. Mean CC thickness overall and mean thickness for defined anatomical segments of the CC were derived by using all the thickness measurements for the CC and all thickness measurements in each segment respectively. Both mean thickness and maximum thickness measurements were compared against brain volume (overall) as well as to grey and white matter volume individually. In addition, thickness and volume were compared against neurodevelopment and laboratory parameters of children with HIV and controls. The parameters included Griffiths mental development scores, time on HAART, CD4 (including nadir CD4) and presence of impaired head growth.

4.1. Meeting the objectives of the study

4.1.1. Comparing corpus callosum thickness and brain volume in children with HIV-related brain disease against 'normal' children and determining which segments of the corpus callosum are most affected

There were no statistically significant differences in CC thickness or brain volume between patients and controls. Patients with HIVE were expected to demonstrate atrophy (i.e. lower volume) (2, 41, 42), and the lack of significant atrophy in patients when compared to controls needs to be explained in the context of the referral criteria, where 'impaired head growth' was one of the three criteria for referral for MRI.

HIV has been associated with a decreased CC thickness in adults but in these studies patients also exhibited decreased brain volumes (4). In contrast, Ances and colleagues in their study of adults with HIV did not find any differences in white matter volume between HIV positive and negative patients, but showed CC thinning in HIV-infected patients (27). Decreased thickness of the CC in children with HIV may not be solely related to Wallerian degeneration-type shrinkage (12) but may occur due to inhibited development (16) or as a direct/indirect effect of HIV on the CC (27) and may therefore occur independently of brain atrophy. The areas of the brain most affected in HIV are reported to be those close to the ventricles. This is thought to be due to 'easier viral penetration resulting from HIV infected mononuclear cells trafficking from cerebrospinal fluid into brain' (4, 27). Supporting this is the finding that the highest HIV concentrations in the brain are in the caudate nuclei and CC (4, 27). Understanding why there was no decrease in brain volume in our patients requires some speculation. Some proposed reasons why the brain volumes of HIV-infected children may be not be decreased include: (a) The increased prevalence of HIV encephalitis in the HAART era (4) may reflect the host response in a form of the Immune Reconstitution Inflammatory Syndrome (IRIS). Oelschlaeger and colleagues reported an adult case where a patient died after a change in antiretroviral therapy. The post mortem examination revealed that the patient had 'diffuse swelling, leptomeningeal infiltration by CD8+ cells and enhancement of perivascular spaces by CD8+ cells' (50). 'Up to 37% of patients may develop IRIS, mainly when HAART is started in antiretroviral-naïve patients, who develop a rapid recovery of immune function' (50). All our patients were on ART at the time of scanning which may account for recovery of brain volume, possibly through inflammation.

(b) Our controls may have decreased brain volume (rather than patients having an increased brain volume) for a number of reasons including malnutrition (51). Our controls were unlikely to be 'normal' subjects as they had been referred for MRI, but they were non-HIV infected children and had no abnormalities detected on scanning. In a population with a high prevalence of malnutrition and chronic disease, radiologists using subjective MRI interpretations, working in local conditions, may not necessarily detect atrophy.
(c) Our patients were selected to reflect 'HIV-related brain disease', rather than 'HIV encephalopathy' which is a more serious condition where there is significant developmental delay (GMDS scores 2 standard deviations below mean). Our patients showed GMDS scores only one standard deviation from the mean.

Segmental CC thickness followed the overall CC thickness when comparing patients with controls, in both means and maximums. The premotor segment was the only part of the CC where thickness correlated significantly with age ($p < 0.05$). The Prefrontal CC correlated the least with age ($p = 0.98$) suggesting stability in thickness over different age groups. The anterior portions of the CC are reported to change the least with age and vary the least between humans, and are therefore proposed for use as a reference point against which the thickness of the posterior portions can be compared (13). Luders et al. confirmed this in 190 children where the most significant thickening of the CC associated with normal development occurred at the splenium and mid-body of the CC, and the least at the rostrum (i.e. prefrontal CC segment) (11).

4.1.2. Correlating corpus callosum thickness with brain volume in children with HIV-related brain disease

Mean thickness measurements for the 'Overall CC' showed a positive correlation with TBV for both patients and controls. Mean segmental thicknesses in the premotor and sensory CC also correlated significantly with TBV, while mean and maximum premotor and maximum prefrontal CC thickness correlated significantly with WMV. These findings are similar to other paediatric studies where CC thickness has been correlated to brain volume. Both Northan et al and Narberhaus et al demonstrated a correlation between CC thinning and decreased brain volume in children (9, 16). Luders et al. also showed thinning of the CC in children with ADHD who had smaller overall brain volumes (17). Hasan and colleagues considered that the CC volumes and their DTI white matter fibre trajectories resembled whole brain volumes (12). These authors mirrored our hypothesis that the CC was an indicator of whole brain volume and volume loss (12). They also proposed the use of CC as a surrogate marker of white matter pathology, as we have done (12). They did not, however, conceive the use of simple linear measures of the CC to replace more complex volumetric assessment in the clinical setting. Simple linear thickness measurement of the corpus callosum, in the context of HIV in children, is a novel way for evaluating white matter and total brain volumes. This will allow for the diagnosis of HIV encephalopathy in an objective way on imaging studies and will also allow assessment of response to appropriate therapy through longitudinal measures of corpus callosum thickness.

4.1.3. Correlating segmental prefrontal corpus callosum thickness with brain volume in children with HIV-related brain disease

For practical use, a radiologist is more likely to utilise a single linear thickness measurement, at one point on a sagittal image of the CC, than to make multiple measurements. A segmental CC thickness that correlated significantly with WMV was the prefrontal segment ($p < 0.05$). Using the 'prefrontal CC thickness' segmental measurement as a surrogate marker of WMV is easy to perform, as this part of the CC is simply identified as the anterior $1/6^{th}$.Of note, this is also the thickest part of the CC in general and is least correlated with patient age (i.e. shows thickness stability over all ages). However, using this as a surrogate marker of brain volume should be undertaken with caution, considering that the correlation between prefrontal CC thickness and WMV had an r-value correlation of 0.35, meaning that only 12% of the variance is explained by the relationship between CC thickness and WMV. Thus 88% is unexplained and there is likely to be huge overlap in CC thickness between normal brain volume and reduced brain volume. Thompson and colleagues showed that selective CC regional (segmental) thinning in adults was associated with volume loss in the portions of the cortex where the fibres project. Volume loss in the frontal regions of the brain was reflected as anterior CC thinning (i.e. prefrontal segment) while the sensorimotor cortical losses were reflected at the mid-body of the CC (4).

The prefrontal segment (maximum) thickness also correlated significantly with the nadir CD4 count ($p<0.05$). CD4 counts are measures of the severity of immunosuppression and the nadir CD4 represents the patients' worst affected period (the lowest point of their immunity during the time of being measured). CD4 counts at the time of investigation

were relatively high for an HIV-infected population (none were below 200), which suggests that the infection was controlled in the study population. This is also a possible reason why there is no major volume loss in the patient population.

4.1.4. Correlation of corpus callosum thickness with mental development scores in children with HIV-related brain disease

Mean scores in patients fell into the 'low average' category, with a mean GQ of 84 (range 72 – 101), 'locomotor' sub-quotient of 84 (range 59 – 116) and the 'language' sub quotient of 80 (range 57 – 118). These mean scores are approximately 1 standard deviation lower than the described GMDS in HIV-**uninfected** children at 21 months of age for this community (with means of 95, 99.7 and 93.2 respectively for GQ, 'locomotor' and 'language') (49). Significant developmental delay is regarded as more than 2 SDs below the mean i.e. quotients lower than 70. This may account for the lack of atrophy in our patients who have not yet manifested the severe developmental delay associated with HIVE-related atrophy.

The CC maximum thickness at the motor segment correlated inversely with the GQ (i.e. a thicker motor CC segment correlated with a lower GQ). Thickness has been proposed to relate to motor / sensory functions (20). Our findings are contrary to what we had expected and are difficult to explain. Other authors have shown that a larger CC size is reportedly 'associated with better motor performance in children born with very low birth weight' (18).

4.1.5. Correlation of corpus callosum thickness and brain volume with laboratory parameters of immunosuppression in children with HIV-related brain disease

A study by Thompson et al. in adults with HIV demonstrated that CC thinning was associated with decreasing CD4 counts (4). They were unable to demonstrate an association between CC thickness and viral load, however. They postulated that this was possibly 'because viral load waxes and wanes in AIDS patients on treatment', and that it is more likely that **viral load in the brain** correlates with brain volume loss rather than viral load in the blood stream. In support of this are reports that the caudate nuclei have the highest viral load and show the worst shrinkage (4). Our only statistically significant correlation to support this was with nadir CD4 and maximum prefrontal CC thickness.

Some studies of HIV-infected patients have shown a correlation of CD4/ nadir CD4 with brain volume (4, 5). Cohen and colleagues' conclusion following a study of 69 HIV-infected adults was that those with a history of chronic HIV infection (as determined by duration since sero-conversion) and with episodes of severely impaired immune function (determined from nadir CD4) are at greatest risk for atrophy (44). We demonstrated no statistical correlation between brain volume and CD4, in line with Ances and colleagues who also did not show any correlation between CD4 and structural measures. They suggested that patients on treatment might develop IRIS (27).

4.1.6. The corpus callosum length and its relationship to clinical findings

CC length investigations were not an intended objective of this study, however, it was noted that the length of the CC was preserved in patients, with no statistical difference

with controls. CC length showed an inverse association with the CD4 closest to the time of the scan (p=0.04). This is difficult to explain unless there is an expected volume gain in our HIV-infected patients relating to treatment with HAART and development of IRIS. However, low CD4 closest to the time of the scan when the length is increased suggests that IRIS is a less plausible explanation for this scenario. It should also be kept in mind that numerous univariate analyses were performed. By chance alone, some of these may produce statistically significant relationships which are in fact spurious.

4.1.7. HAART may be neurotoxic

The CHER study in South Africa showed the benefits of immediate ART in children with HIV (52) and the WHO recommends ART for all HIV-infected children under two years of age (53). Safety and dose of many important anti-retrovirals used in adults have not been determined for children (53). Becker and colleagues showed significant atrophy of the corpus striatum in adults with HIV treated with HAART. In these patients, the atrophy was related to the length of time they had been diagnosed as sero-positive. The authors suggested that either atrophy is a chronic subclinical process occurring despite treatment, or that the extent of the **initial insult** dictated the extent of the atrophy (45). Other work in adults has suggested that the drug Efavirenz, used as part of HAART, may itself be neurotoxic. Cicarrelli and colleagues showed a significant risk of cognitive impairment in adults on cART (54). In our study, there were no significant correlations with time on HAART and none of our patients were treated with Efavirenz.

4.1.8. Other studies of corpus callosum thickness measurement

Studies published in the last 8 years (2007 - 2014) that involve CC thickness measurements include three studies performed exclusively in children (8, 17, 55), two studies that included a combination of children and adults (11, 20) and two studies researching the long-term effects of neonatal diseases by imaging exclusively adolescents (9, 16). These are summarised in Table 4.1, alongside results from the current study. Luders et al showed that unlike adults, who show a positive correlation between CC thickness and intelligence (7), children show a negative correlation between CC thickness and intelligence (20). However, these studies did not speculate on when the transition to adulthood occurs. These age-related physiological processes may account for some of the differences encountered in children and may account for some of the inverse correlations of CC thickness and GMDS that were found in the current study.

Many positive pathological correlations have been made with decreased CC thickness in children in the past (Table 4.1) including hydrocephalus, mental retardation, sickle cell disease, spastic quadraparesis, fetal alcohol syndrome (FAS), medulloblastoma with leukaemia and preterm birth (20). More recently, both Narberhaus (9) and Northam (16) showed decreased CC thickness in adolescents who were born prematurely and correlated this with a lower IQ. They also correlated CC thinning with decreased brain volume (9, 16). Luders showed thinning of the CC in children with ADHD, together with smaller overall brain volumes (17). Yang correlated FAS with thinning of the CC, which was especially prominent at the anterior third of the CC in the South African cohort of children included in the study (8).

Table 4.1. Comparison of research of corpus callosum thinning spanning 2007 – 2014 (7-9, 11, 12, 16, 17, 20, 27, 55)

Study	No of subjects (patients)	Children Adolescents Adults	Method described by Luders et al 2007	Findings
Northam 2011	49	Adolescents	No	Preterms: decreased WMV and thinned CC Thinning of CC: 8 point IQ drop
Yang 2011	153	Children	Yes	FAS :thinning of anterior third of CC, especially the South African cohort, and thinning of splenium
Narberhaus 2007	64	Adolescents	No	Prems < 27 weeks have long term CC and WM abnormality with lower IQ (splenium correlates best with IQ)
Luders 2007	62	Adults	Yes	Positive correlation between CC thickness and intelligence
Hasan 2009	?	?	No	Insignificant gender effect on volume of CC or its subsections
Ances 2012	78	Adults	No	HIV resulted in decreased brain volume, including volume of CC
Luders 2010	190	Children	Yes	Developing CC increases in thickness except for rostrum in females Most growth occurs in splenium and midbody
Luders 2009	38 (19 patients)	Children	Yes	CC significantly thinner in ADHD but also smaller brain volumes than controls
Westerhausen 2011	20	Children	Yes	Increasing thickness of isthmus showed less interhemispheric transfer.
Luders 2011	200	Children Adolescents (6-17yrs)	Yes	Negative correlation between thickness and intelligence in children (opposite to adults Luders 2007)
Andronikou 2012	44 (33 patients)	Children	No	Correlation CC thickness and total/white matter volume Correlation prefrontal CCthickness with time on HAART and CD4 count Correlation of motor CC segment and general mental development quotient

Key to abbreviations: WM = white matter; CC= Corpus Callosum; IQ = intelligence quotient; FAS = Fetal alcohol syndrome; Prems= premature neonates; HIV = human immunodeficiency virus; ADHD = attention deficit hyperactivity disorder; HAART = highly active anti-retroviral therapy

4.2. Current applications

4.2.1 Semi-automated method of measuring corpus callosum thickness

The group of Luders introduced a semi-automated tool for measuring the CC thickness in 2007 (7) and this has subsequently been used in a number of research projects (7, 8, 11, 17, 20, 55) . The method is very similar to the customised tool used in the current study but offers 100 segment measurements compared to the 40 used here, which results in a higher spatial resolution and more detailed results than the current study. Our custom tool was designed for use with DTI images where the segments would serve as seeds from the midpoint for white matter fibre tracking (47). The 40 segments were chosen specifically to ensure that each segment still consists of a contiguous strip of voxels across the CC from the dorsal to the ventral contour for DTI image resolution. The custom tool will be used in future research involving fibre tracking, both for segmenting the CC accurately and for estimating the number of fibres in the hemispheres.

4.3. Limitations of the current study

4.3.1. Sample limitations

The main limitation of this research is the sample number, which decreased significantly due to exclusions. A total of 48 dedicated MRI scans were performed in children with HIV-related brain disease at the research facility at Cross Universities Brain Imaging Centre (CUBIC), as part of the larger study. The lack of a formal patient archiving and

communications system (PACS) at the time of the research meant that MRI scans had to be recorded and stored on DVD which led to loss of imaging data. Further cases had to be excluded as the imaging data were degraded by movement artefact to such a degree that volume analysis became unusable. A total of 15 patients and five controls were excluded in total, severely affecting the total numbers of the study group.

Users of automated brain volume programs such as the SPM package used in this study are advised to manually inspect the output to ensure that the results are accurate and reliable (3), and to remove or correct those cases where the output is flawed. These recommendations were adhered to in the current study. It should also be kept in mind that the accuracy of such techniques is dependent on 'image quality, scan parameters and scanning hardware' (3). Image quality is often degraded in children who have difficulty remaining still for the duration of MRI. Similar problems are encountered in unsedated imaging, especially in research where anaesthesia is considered an unwarranted risk.

4.3.2. Limitations relating to controls

Control patients that are age matched are difficult to obtain without resorting to scanning normal subjects. The need for anaesthesia in children under 6 years of age (our patient mean age was 31 months / median 30 months) undergoing MRI scanning precluded scanning normal children because of the risks involved. Using scans of patients imaged for other indications in the same population group, that are reported as normal by the clinical radiologists, is a flawed technique for generating controls as this does not

necessarily prove that patients were normal and does not account for the reason for these children being referred in the first place.

4.3.3. Limitations to comparing with published research

The variation of our results from those in the literature may have resulted from differing sample sizes, composition of subjects (gender, age and population group) and methods used for quantifying the CC and white matter volume (11).

4.3.4. Technical limitations of corpus callosum thickness measurement

The semi-automated technique of CC thickness measurement has some technical limitations related to it, as well as the possibility of variation in operator-dependent steps.

(a) Selection of the appropriate midline slice for use is subjective and may not actually represent the true midline of the patient. It is also dependent on the thickness and number of routine MRI slices available. This is, however, the reality of practice in radiology.

(b) Drawing the margins of the CC is a partly manual function of the operator (the principal investigator in this case). This involves depositing multiple points using the cursor along the superior and inferior margins of the CC, which are joined by the computer software. The number of points to be placed and the exact location of the placements were not strictly defined, resulting in variation in this aspect. The following limitations were found when performing this task:

(i) The inferior CC margin is not as distinct as the superior margin.

(ii) The rostral edge is often indistinct.

(iii) The region of the union of the fornix with the CC makes the inferior margin difficult to identify.

(iv) Start and end-points (i.e. the mid rostral and mid splenial start points) were randomly selected – there is no anatomical landmark for these.

(v) The point deposition may be inaccurate due to the physical thickness of the cursor point itself - this plays a role at the thinnest portion of the CC (the isthmus).

(c) Inter-observer/operator agreement:

ICC is interpreted similarly to correlation. It is always difficult to say what is good agreement and what is poor agreement, because it is relative.

The SEM can be seen as a measure of the expected difference between the operators expressed in the same units as the measurements.

We therefore interpret our results as good agreement on overall CC thickness and prefrontal thickness, moderate agreement on premotor, motor, and visual thickness and poor agreement on overall length measurement. Therefore, even with the use of a semi-automated tool, the manual placement of cursors can result in differences between operators, as is the case with any measurement performed manually by a radiologist.

(d) Limitations of CC segmentation based on proportion: The only true way of determining which portions of the CC represent specific crossing white matter fibres is through the use of DTI with fibre tracking. As DTI was not available at the time of imaging, we divided the length of the CC proportionally. This method was chosen for the current

study rather than anatomical division of the segments, as it was suspected that anatomical boundaries specifically distinguishable by their thickness (such as the isthmus) may have been affected by disease in varying proportions.

4.3.5. Structural vs. physiological assessment

A major limitation to the above work is that it remains a structural assessment of the brain. New MRI technology including DTI, MR spectroscopy, functional MRI and perfusion MRI can determine white matter integrity levels, metabolites, loss of function and blood flow abnormalities in HIV. These modalities may be more illuminating of the disease process, as physiological change probably precedes structural change.

4.4. Future applications

Follow-up work is in progress including techniques that provide information on white matter fibre integrity (fractional anisotropy) and white matter fibre numbers, as well as CC segmentation based on white matter tractography projections from relevant lobes of the brain. This is all achievable through DTI, however, these techniques are more expensive, time consuming and often unavailable for use in our current clinical settings. In contrast, linear measurements of CC thickness are available off routine sagittal T1-weighted MRI, using the measurement callipers, at no additional cost.

Additional future research is recommended to correlate patients with measurable brain volume losses in HIV and CC thickness. Refinements in MRI sequences, which include the motion correcting sequences that allow patients to undergo scanning without

anaesthesia risks, will yield larger groups of patients with usable data, and true ‘normal subjects’ as controls.

The technical limitations related to placement of cursors in the semi-automated method may be obviated by a fully automated method. Developing such a software package should include clear definitions for each step of midline selection, cursor placement number and position.

5. Conclusion

This research has met its objectives in demonstrating a statistically significant, albeit weak, correlation between CC thickness and brain volume, even though patients were not shown to have significantly diminished brain volumes as compared to controls.

The prefrontal CC is the most convenient and robust area for any visual assessment or 'spot' measurements because this is easily identified as the anterior $1/6^{th}$, is the thickest part of the CC and changes least with age.

Although the maximum thickness of the prefrontal segment of the CC also showed a statistically significant correlation with nadir CD4 (which is the lowest point of immunity measured for a patient), we have not demonstrated significant clinical usefulness of for CC thickness in our patients.

Appendix A: White Matter Signal Abnormalities in Children with Suspected HIV-related Neurologic Disease on Early Combination Antiretroviral Therapy

The following is the article as it appeared in print in The Pediatric Infectious Disease Journal in August 2014

Appendix B: Letter of contribution by first author

Appendix C: A semi-automated method for measuring thickness and white matter integrity of the corpus callosum

The following is the article as it appeared in print in the South African Journal of Radiology

December 2012

Appendix D: Corpus callosum thickness in children: an MR pattern-recognition approach on the midsagittal image

The following is the article as it appeared in the journal 'Pediatric Radiology' in issue 45 in 2015.

Appendix E: Correlating brain volume and callosal thickness with clinical and laboratory indicators of disease severity in children with HIV-related brain disease

The following is the article as it appeared in print in the journal 'Childs Nervous System' in issue 30 in 2014.

Appendix F: Corpus Callosum Thickness on Mid-sagittal MRI as a Marker of Brain Volume: A pilot Study in Children with HIV Related Brain Disease and Controls

The following is the article as it was published in the journal 'Pediatric Radiology' in issue 45 in 2015.

Appendix G: Oral Presentation Athens 2012

49th Annual Meeting of the European Society of Paediatric Radiology

Friday 1 Jun 2012

11:21-11:31 88 - LP: **Corpus callosum thickness on MRI as a surrogate marker of white matter volume in children with HIV and its correlation with developmental scores**

Savvas Andronikou[1], Christelle Ackermann[2], Barbara Laughton[2], Els Dobbels[2], Steve Innes[2], Reghana Taliep[2], Ronald van Toorn[2], Mark Cotton[2], Bruce Spottiswoode[3], John Pettifor[1]
[1]University of the Witwatersrand, Johannesburg; [2]University of Stellenbosch; [3]University of Cape (South Africa)

Appendix H: Poster ESPR 2010, 7-11 June 2010, Bordeaux France

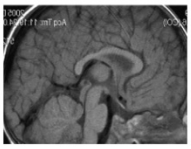
CORPUS CALLOSUM THICKNESS MEASURMENT: a semi-automated method for inferring white matter volume loss

Savvas Andronikou[1], Bruce S. Spottiswoode[2,3]

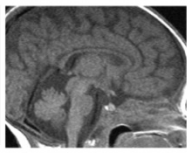
[1]Department of Radiology, Faculty of Health Sciences, University of The Witwatersrand, South Africa
[2]Department of Human Biology, Faculty of Health Sciences, University of Cape Town, South Africa
[3]Department of Radiology, Faculty of Health Sciences, Stellenbosch University, South Africa

What's the idea?

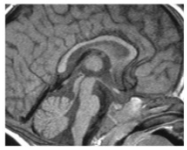
Corpus callosum thickness is a surrogate marker of overall white matter volume loss. We designed and tested a customized semi-automated tool for measuring the corpus callosum (CC) thickness and plotting this as a function of CC length. Uses include development of a normal range for comparison to patients with white matter loss. It also allows determination of the topographically affected components of the CC.



Normal CC at 6 months. Note the thickness due to myelination - white on T1



Normal CC at birth before myelination. Note the thin CC and low signal on T1

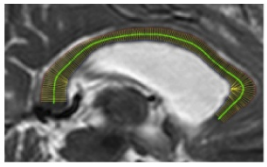


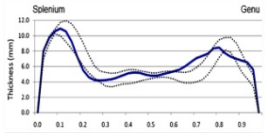
An older child with WM atrophy demonstrates a thin posterior CC

Methods

Six normal volunteers and one patient with multiple sclerosis were scanned on a 3T MRI system (Siemens MAGNETOM Allegra). Sagittal images were imported into a custom tool written in MATLAB (The Mathworks Inc, Natick, MA). The midline sagittal position was identified and the corpus callosum (CC) was parcellated as follows: dorsal and ventral CC contours were manually drawn and the CC was divided by the software into segments equally spaced with reference to a contour placed midway between the dorsal and ventral contours. These segments can then be plotted as a function of normalized distance along the midline contour. A patient with pathology can then be identified relative to a normal range for a specific age. Sagittal Diffusion Tensor Imaging images were used and each segment was designed to act as a seed for fiber tracking - future research is intended to plot CC fractional anisotropy values and fiber quantity.

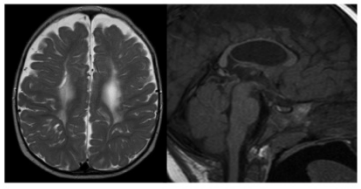
Results



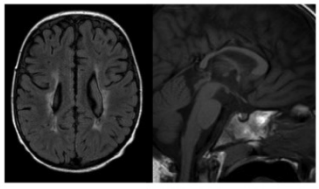


Conclusion: The system successfully demonstrated regional CC thickness in normal patients providing a normal range (dotted lines) and confirming the patient with pathology (solid line).

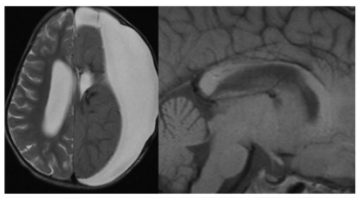
Suggested uses



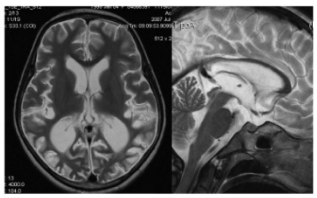
Global Hypoxia WM loss – diffusely thin CC



PVL – predominantly thin splenium of CC



Unilateral infarct – focally thin central CC



WM loss in HIV - diffusely thin CC

Appendix I: Ethics clearance certificate

UNIVERSITY OF THE WITWATERSRAND, JOHANNESBURG
Division of the Deputy Registrar (Research)

HUMAN RESEARCH ETHICS COMMITTEE (MEDICAL)
R14/49 Professor Savvas Andronikou

CLEARANCE CERTIFICATE	M110802
PROJECT	Corpus Callosum Thickness on MRI as a Surrogate Marker of White Matter Volume in Children with HIV Encephalopathy and Correlation with Developmental Scores
INVESTIGATORS	Professor Savvas Andronikou.
DEPARTMENT	Radiology Department
DATE CONSIDERED	26/08/2011
M1108020DECISION OF THE COMMITTEE*	Approved unconditionally

Unless otherwise specified this ethical clearance is valid for 5 years and may be renewed upon application.

DATE 07/09/2011 **CHAIRPERSON** .....
(Professor PE Cleaton-Jones)

*Guidelines for written 'informed consent' attached where applicable
cc: Supervisor : Professor John Pettifor

DECLARATION OF INVESTIGATOR(S)

To be completed in duplicate and **ONE COPY** returned to the Secretary at Room 10004, 10th Floor, Senate House, University.
I/We fully understand the conditions under which I am/we are authorized to carry out the abovementioned research and I/we guarantee to ensure compliance with these conditions. Should any departure to be contemplated from the research procedure as approved I/we undertake to resubmit the protocol to the Committee. **I agree to a completion of a yearly progress report.**

PLEASE QUOTE THE PROTOCOL NUMBER IN ALL ENQUIRIES...

6. References

1. Tucker K A, Robertson K R, Lin W, Smith J K, An H, Chen Y, et al. Neuroimaging in human immunodeficiency virus infection. Journal of neuroimmunology. 2004;157:153-162.

2. Gavin P, Yogev R. Central nervous system abnormalities in pediatric human immunodeficiency virus infection. Pediatric neurosurgery. 1999;31:115-123.

3. Dewey J, Hana G, Russell T, Price J, McCaffrey D, Harezlak J, et al. Reliability and validity of MRI-based automated volumetry software relative to auto-assisted manual measurement of subcortical structures in HIV-infected patients from a multisite study. NeuroImage. 2010;51:1334-1344.

4. Thompson P M, Dutton R A, Hayashi K M, Lu A, Lee S E, Lee J Y, et al. 3D mapping of ventricular and Corpus Callosum abnormalities in HIV/AIDS. NeuroImage. 2006;31:12-23.

5. Chiang M C, Dutton R A, Hayashi K M, Lopez O L, Aizenstein H J, Toga A W, et al. 3D pattern of brain atrophy in HIV/AIDS visualized using tensor-based morphometry. NeuroImage. 2007;34:44-60.

6. Giedd J N, Rumsey J M, Castellanos F X, Rajapakse J C, Kaysen D, Vaituzis A C, et al. A quantitative MRI study of the Corpus Callosum in children and adolescents. Brain research Developmental brain research. 1996;91:274-280.

7. Luders E, Narr K L, Bilder R M, Thompson P M, Szeszko P R, Hamilton L, et al. Positive correlations between Corpus Callosum thickness and intelligence. NeuroImage. 2007;37:1457-1464.

8. Yang Y, Phillips O R, Kan E, Sulik K K, Mattson S N, Riley E P, et al. Callosal thickness reductions relate to facial dysmorphology in fetal alcohol spectrum disorders. Alcoholism, clinical and experimental research. 2012;36:798-806.

9. Narberhaus A, Segarra D, Caldu X, Gimenez M, Junque C, Pueyo R, et al. Gestational age at preterm birth in relation to Corpus Callosum and general cognitive outcome in adolescents. Journal of child neurology. 2007;22:761-765.

10. Garel C, Cont I, Alberti C, Josserand E, Moutard M L, Ducou le Pointe H. Biometry of the Corpus Callosum in children: MR imaging reference data. AJNR American journal of neuroradiology. 2011;32:1436-1443.

11. Luders E, Thompson P M, Toga A W. The development of the Corpus Callosum in the healthy human brain. The Journal of neuroscience : the official journal of the Society for Neuroscience. 2010;30:10985-10990.

12. Hasan K M, Kamali A, Iftikhar A, Kramer L A, Papanicolaou A C, Fletcher J M, et al. Diffusion tensor tractography quantification of the human Corpus Callosum fiber pathways across the lifespan. Brain research. 2009;1249:91-100.

13. Wilde E A, Chu Z, Bigler E D, Hunter J V, Fearing M A, Hanten G, et al. Diffusion tensor imaging in the Corpus Callosum in children after moderate to severe traumatic brain injury. Journal of neurotrauma. 2006;23:1412-1426.

14. Hofer S, Frahm J. Topography of the human Corpus Callosum revisited--comprehensive fiber tractography using diffusion tensor magnetic resonance imaging. NeuroImage. 2006;32:989-994.

15. Dougherty R F, Ben-Shachar M, Deutsch G, Potanina P, Bammer R, Wandell B A. Occipital-callosal pathways in children: Validation and atlas development. Annals of the New York Academy of Sciences. 2005;1064:98-112.

16. Northam G B, Liegeois F, Chong W K, Wyatt J S, Baldeweg T. Total brain white matter is a major determinant of IQ in adolescents born preterm. Annals of neurology. 2011;69:702-711.

17. Luders E, Narr K L, Hamilton L S, Phillips O R, Thompson P M, Valle J S, et al. Decreased callosal thickness in attention-deficit/hyperactivity disorder. Biological psychiatry. 2009;65:84-88.

18. Skranes J, Vangberg T R, Kulseng S, Indredavik M S, Evensen K A, Martinussen M, et al. Clinical findings and white matter abnormalities seen on diffusion tensor imaging in adolescents with very low birth weight. Brain : a journal of neurology. 2007;130:654-666.

19. Stewart A L, Rifkin L, Amess P N, Kirkbride V, Townsend J P, Miller D H, et al. Brain structure and neurocognitive and behavioural function in adolescents who were born very preterm. Lancet. 1999;353:1653-1657.

20. Luders E, Thompson P M, Narr K L, Zamanyan A, Chou Y Y, Gutman B, et al. The link between callosal thickness and intelligence in healthy children and adolescents. NeuroImage. 2011;54:1823-1830.

21. Yung A P, G.; Qui, D. et al. White Matter Volume and Anisotropy in Preterm Children: a Pilot Study of Neurocognitive Correlates. Pediatric Rsearch. 2004;61:1-5.

22. Georgy B A, Hesselink J R, Jernigan T L. MR imaging of the Corpus Callosum . AJR American journal of roentgenology. 1993;160:949-955.

23. Osborn A G, Ross J S, Salzman K L, al e. Expertddx: Brain and spine. 1 edition ed: Lippincott Williams & Wilkins; 2008.

24. Ho M L, Moonis G, Ginat D T, Eisenberg R L. Lesions of the Corpus Callosum . AJR American journal of roentgenology. 2013;200:W1-16.

25. STATdx. [DOI26 June 2013]; Available from: https://my.statdx.com/STATdxMain.jsp rc=false#edxExpandedContent;thin_corpus_callosum_expert-ddx1.

26. Barkovich A J, Raybaud C, editors. Pediatric Neuroimaging Fifth edition ed: Lippincott Williams & Wilkins; 2011.

27. Ances B M, Ortega M, Vaida F, Heaps J, Paul R. Independent effects of HIV, aging, and HAART on brain volumetric measures. J Acquir Immune Defic Syndr. 2012;59:469-477.

28. Lane J I, Luetmer P H, Atkinson J L. Corpus callosal signal changes in patients with obstructive hydrocephalus after ventriculoperitoneal shunting. AJNR American journal of neuroradiology. 2001;22:158-162.

29. Mitchell W. Neurological and developmental effects of HIV and AIDS in children and adolescents. Mental retardation and developmental disabilities research reviews. 2001;7:211-216.

30. Fowler M G. Pediatric HIV infection: neurologic and neuropsychologic findings. Acta Paediatr Suppl. 1994;400:59-62.

31. Sanchez-Ramon S, Resino S, Bellon Cano J M, Ramos J T, Gurbindo D, Munoz-Fernandez A. Neuroprotective effects of early antiretrovirals in vertical HIV infection. Pediatric neurology. 2003;29:218-221.

32. Schmitt B, Seeger J, Kreuz W, Enenkel S, Jacobi G. Central nervous system involvement of children with HIV infection. Developmental medicine and child neurology. 1991;33:535-540.

33. Czornyj L A. [Encephalopathy in children infected by vertically transmitted human immunodeficiency virus]. Revista de neurologia. 2006;42:743-753.

34. Shanbhag M C, Rutstein R M, Zaoutis T, Zhao H, Chao D, Radcliffe J. Neurocognitive functioning in pediatric human immunodeficiency virus infection: effects of combined therapy. Archives of pediatrics & adolescent medicine. 2005;159:651-656.

35. Pomara N, Crandall D T, Choi S J, Johnson G, Lim K O. White matter abnormalities in HIV-1 infection: a diffusion tensor imaging study. Psychiatry research. 2001;106:15-24.

36. Thurnher M M, Schindler E G, Thurnher S A, Pernerstorfer-Schon H, Kleibl-Popov C, Rieger A. Highly active antiretroviral therapy for patients with AIDS dementia complex: effect on MR imaging findings and clinical course. AJNR American journal of neuroradiology. 2000;21:670-678.

37. States L J, Zimmerman R A, Rutstein R M. Imaging of pediatric central nervous system HIV infection. Neuroimaging clinics of North America. 1997;7:321-339.

38. Angelini L, Zibordi F, Triulzi F, Cinque P, Giudici B, Pinzani R, et al. Age-dependent neurologic manifestations of HIV infection in childhood. Neurological sciences : official journal of the Italian Neurological Society and of the Italian Society of Clinical Neurophysiology. 2000;21:135-142.

39. Kollar K, Jelenik Z, Hegelsberger E. [Neurologic aspects of HIV infections--follow-up of pediatric patients]. Ideggyogyaszati szemle. 2003;56:397-404.

40. Patsalides A D, Wood L V, Atac G K, Sandifer E, Butman J A, Patronas N J. Cerebrovascular disease in HIV-infected pediatric patients: neuroimaging findings. AJR American journal of roentgenology. 2002;179:999-1003.

41. Spreer J, Enenkel-Stoodt S, Funk M, Fiedler A, de Simone A, Hacker H. [Neuroradiological findings in perinatally HIV-infected children]. RoFo : Fortschritte auf dem Gebiete der Rontgenstrahlen und der Nuklearmedizin. 1994;161:106-112.

42. Johann-Liang R, Lin K, Cervia J, Stavola J, Noel G. Neuroimaging findings in children perinatally infected with the human immunodeficiency virus. The Pediatric infectious disease journal. 1998;17:753-754.

43. Kauffman W M, Sivit C J, Fitz C R, Rakusan T A, Herzog K, Chandra R S. CT and MR evaluation of intracranial involvement in pediatric HIV infection: a clinical-imaging correlation. AJNR American journal of neuroradiology. 1992;13:949-957.

44. Cohen R A, Harezlak J, Schifitto G, Hana G, Clark U, Gongvatana A, et al. Effects of nadir CD4 count and duration of human immunodeficiency virus infection on brain volumes in the highly active antiretroviral therapy era. Journal of neurovirology. 2010;16:25-32.

45. Becker J T, Sanders J, Madsen S K, Ragin A, Kingsley L, Maruca V, et al. Subcortical brain atrophy persists even in HAART-regulated HIV disease. Brain imaging and behavior. 2011;5:77-85.

46. Griffiths R. The Griffiths Mental Development Scales, from birth to 2 years. Oxford: Association for research in infant and child development. The Test Agency; 1996 [updated The 1996 Revision by Michael Huntley. ; cited 2013 January 7th]; Available from: http://www.hogrefe.co.uk/griffiths-mental-development-scales-revised-birth-to-2-years-gmds-0-2.html.

47. Andronikou S, Spottiswoode B S, Tomazos N. A semi-automated method for measuring thickness and white matter integrity of the Corpus Callosum . South African Journal of Radiology 2012;16:130 - 133.

48. Luiz D, Faragher, B., Barnard, A. Griffiths mental development Scales – Extended Revised, two to eight years. Oxford: Association for research in infant and Child Development. The Test Agency; [cited 2013 January 7th]; Available from:

http://www.hogrefe.co.uk/griffiths-mental-development-scales-extended-revised-2-to-8-years-gmds-er-2-8.html.

49. Laughton B, Springer P, Grove D, Seedat S, Cornell M, Kidd M, et al. Longitudinal developmental profile of children from low socio-economic circumstances in Cape Town, using the 1996 Griffiths Mental Development Scales. SAJCH : the South African journal of child health. 2010;4:106-111.

50. Oelschlaeger C, Dziewas R, Reichelt D, Minnerup J, Niederstadt T, Ringelstein E B, et al. Severe leukoencephalopathy with fulminant cerebral edema reflecting immune reconstitution inflammatory syndrome during HIV infection: a case report. Journal of medical case reports. 2010;4:214.

51. Atalabi O M, Lagunju I A, Tongo O O, Akinyinka O O. Cranial magnetic resonance imaging findings in kwashiorkor. The International journal of neuroscience. 2010;120:23-27.

52. Violari A, Cotton M F, Gibb D M, Babiker A G, Steyn J, Madhi S A, et al. Early antiretroviral therapy and mortality among HIV-infected infants. The New England journal of medicine. 2008;359:2233-2244.

53. Lallemant M, Chang S, Cohen R, Pecoul B. Pediatric HIV--a neglected disease? The New England journal of medicine. 2011;365:581-583.

54. Ciccarelli N, Fabbiani M, Di Giambenedetto S, Fanti I, Baldonero E, Bracciale L, et al. Efavirenz associated with cognitive disorders in otherwise asymptomatic HIV-infected patients. Neurology. 2011;76:1403-1409.

55. Westerhausen R, Luders E, Specht K, Ofte S H, Toga A W, Thompson P M, et al. Structural and functional reorganization of the Corpus Callosum between the age of 6 and 8 years. Cereb Cortex. 2011;21:1012-1017.